23. Y. Tabata and Y. Ikada, *Biomaterials* **20**, 2169 (1999).
24. M. Yamamoto, Y. Tabata, L. Hong, S. Miyamoto, N. Hashimoto and Y. Ikada, *J. Control. Rel.* **64**, 133 (2000).
25. L. Hong, Y. Tabata, S. Miyamoto, K. Yamada, I. Aoyama, M. Tamura, N. Hashimoto and Y. Ikada, *Tissue Eng.* **6**, 331 (2000).
26. M. Ozeki, T. Ishii, Y. Hirano and Y. Tabata, *J. Drug Target.* **9**, 461 (2001).
27. M. Yamamoto, Y. Takahashi and Y. Tabata, *Biomaterials* **24**, 4375 (2003).
28. P. J. Flory, *Principles of Polymer Chemistry*. Cornell University Press, New York, NY (1953).
29. V. Charulatha and A. Rajaram, *J. Biomed. Mater. Res.* **36**, 478 (1997).
30. A. E. Bolton and W. M. Hunter, *Biochem. J.* **133**, 529 (1973).
31. A. Bigi, G. Cojazzi, S. Panazavolta, K. Rubini and N. Roveri, *Biomaterials* **22**, 763 (2001).
32. L. H. H. O. Damink, P. J. Dijkstra, M. J. A. van Luyn, P. B. van Wachem, P. Nieuwenhuis and J. Feijen, *J. Mater. Sci. Mater. Med.* **6**, 460 (1995).
33. H. Ueda, T. Nakamura, M. Yamamoto, N. Nagata, S. Fukuda, Y. Tabata and Y. Shimizu, *J. Control. Rel.* **88**, 55 (2003).
34. K. S. Weadock, E. J. Miller, E. L. Keuffel and M. G. Dunn, *J. Biomed. Mater. Res.* **32**, 221 (1996).
35. K. S. Weadock, E. J. Miller, L. D. Bekkincampi, J. P. Zawadsky and M. G. Dun, *J. Biomed. Mater. Res.* **29**, 1373 (1995).
36. J. E. Lee, J. C. Park, Y. S. Hwang, J. K. Kim, J. G. Kim and H. Sub, *Yonsei Med. J.* **42**, 172 (2001).
37. N. A. Peppas (Ed.), *Hydrogels in Medicine and Pharmacy. Volume II Polymers*. CRC Press, Boca Raton, FL (1987).
38. T. Fujisato, K. Tomihata, Y. Tabata, Y. Iwamoto, K. Burczak and Y. Ikada, *J. Biomater. Sci. Polymer Edn* **10**, 1171 (1999).
39. C. M. Ofner III and W. A. Bubnis, *Pharm. Res.* **13**, 1821 (1996).
40. P. K. Watler, C. H. Cholakis and M. V. Sefton, *Biomaterials* **9**, 150 (1988).
41. P. Dalev, E. Vassileva, J. E. Mark and S. Fakirov, *Biotechnol. Tech.* **12**, 889 (1998).
42. A. A. Apostolov, D. Boneva, E. Vassileva, J. E. Mark and S. Fakirov, *J. Appl. Polym. Sci.* **76**, 2041 (2000).
43. K. Tomihata, K. Burczak, K. Shiraki and Y. Ikada, in: *Polymers of Biological and Biomedical Significance*, S. W. Shalaby, Y. Ikada, R. Langer and J. Williams (Eds), p. 275. American Chemical Society, Washington, DC (1994).
44. Y. Tabata, A. Nagano and Y. Ikada, *Tissue Eng.* **5**, 127 (1999).

Gene Therapy (2005) 12, 857–861

www.nature.com/gt

BRIEF COMMUNICATION

Beta defensin-3 engineered epidermis shows highly protective effect for bacterial infection

D Sawamura[1], M Goto[1], A Shibaki[1], M Akiyama[1], JR McMillan[1], Y Abiko[2] and H Shimizu[1]
[1]*Department of Dermatology, Hokkaido University Graduate School of Medicine, Sapporo; and* [2]*Department of Oral Pathology, Health Sciences University of Hokkaido, Ishikari-Tobetsu, Japan*

Defensins are small cationic proteins that harbor broad-spectrum microbicidal activity against bacteria, fungi and viruses. This study examines the effects on pathogens of the epidermis engineered to express human beta-defensin 3 (HBD3) to combat bacterial infections. First, we examined the localization of HBD3 in the epidermis and observed HBD3 in the intercellular spaces and lamellar bodies of the upper epidermal layers. This result showed HBD3 expressed and assembled in the outer layers of the epidermis was suspected to counter the invading microorganisms. Next, we established a keratinocyte cell line that stably expressed HBD3 and found that the culture medium showed antibacterial activity. Furthermore, we prepared an epidermal sheet of these cells with the HBD3 gene and grafted this onto a dermal wound on a nude rat. The HBD3 engineered epidermis demonstrated significant antimicrobial activity. Skin ulcers without epidermis are constantly exposed to invading microorganisms. Biopsy samples of re-epithelizing epidermis from patients with skin ulcers were collected, and HBD3 mRNA level measured in the epidermis. The epidermal samples from the ulcer skin expressed 2.5 times higher levels of HBD3 transcript than those in the control skin. These results, taken together, indicate that the therapeutic introduction of the HBD3 gene into somatic cells may provide a new gene therapy strategy for intractable infectious diseases.
Gene Therapy (2005) **12,** 857–861. doi:10.1038/sj.gt.3302472; Published online 24 February 2005

Keywords: *keratinocyte; skin; infectious disease; psoriasis*

The skin is always exposed to invading microorganisms, and is accordingly armed with several efficient defence systems. The synthesis of small, antimicrobial peptides was discovered within the last decade and these peptides are highly effective in directly killing microorganisms. The small (3–5 kDa) cationic defensins represent a critical peptide group among a growing number of microbicidal peptides that are capable of a broad spectrum of antimicrobial activity against many Gram-negative and Gram-positive bacteria, fungi, and certain viruses.[1,2]

Mammal defensins comprise genetically distinct α- and β-subfamilies of cationic tri-disulfide bridges. In humans, four types of human β-defensins (HBD), HBD1 through to 4 have been characterized thus far.[3–6] HBD1, 2 and 3 have been identified in human skin and keratinocytes. HBD1 was initially isolated from hemofiltrates[3] and found to be constitutively expressed in various epithelia.[7] However, HBD1 does not appear as abundantly in the epidermis and is not upregulated in response to inflammation as are the other defensins.[5] HBD2 was isolated from the skin of patients with psoriasis and its expression was found in epithelial cells of the skin and the lung. HBD2 is inducible upon treatment with proinflammatory cytokines including TNF-α and interleukin 1, and when in contact with *Pseudomonas aeruginosa* bacteria.[8] HBD3 has also been isolated from psoriatic skin.[5] HBD1 and HBD2 shows antimicrobial activity predominantly against Gram-negative bacteria and these peptides are inactivated in physiologic salt concentrations, while HBD3 has a salt-insensitive broad spectrum activity that kills both Gram-negative and -positive bacteria including *P. aeruginosa*, *Streptococcus pyogenes*, multiresistant *Staphylococcus aureus*, and vancomycin-resistant *Enterococcus faecium*.

The use of conventional antibiotics provides the most powerful means to treat bacterial infections. However, the development of bacterial resistance against conventional antibiotics has emerged as a major public health concern. The appearance of resistant bacteria has been directly linked to the misuse and overuse of antibiotics in humans as well as in farm animals. This situation calls for the development of alternative strategies and therapies to fight infection. Defensins may turn out to be antibacterial agents with low susceptibility to resistance mechanisms, and thus gene therapy using these or the related genes is of great potential for treating intractable infectious diseases.[9–11]

As mentioned above, HBD3 is salt-insensitive and is effective for Gram-positive bacteria, which are common cause of the skin infection. In this study, we introduced the HBD3 gene into a keratinocyte cell line and prepared the epidermal graft overexpressing HBD3 to determine the usefulness or feasibility of HBD3 engineered epidermis as a novel antibacterial therapy.

Correspondence: Professor D Sawamura, Department of Dermatology, Hokkaido University Graduate School of Medicine, N15 W7, Sapporo 060-8638, Japan
Received 4 August 2004; accepted 22 December 2004; published online 24 February 2005

We first examined the localization of HBD3 in normal human control skin. Immunohistochemical analysis demonstrated that HBD3 was located predominantly in the upper spinous and granular layers of the epidermis (Figure 1a). Immunoelectron microscopy showed gold particles in the intercellular spaces of the stratum corneum (Figure 1b). Additionally, gold staining was observed in intracellular membrane-bound vacuoles, close to the apical surface of the granular layer plasma membrane presumed to be lamellar bodies (Figure 1c). Also we used cathepsin D antibodies as control, because cathepsin D is a well-known component localized within lamellar bodes.[12,13] Immunoelectron microscopy of similar sections (Figure 1d) stained with both these antibodies showed that cathepsin D was also expressed within the lamellar body-like membrane-bound vacuoles just beneath the apical granular layer plasma membrane similar to HBD3.

Recently, HBD2 has also been shown to localize to the lamellar bodies and keratinocyte intercellular spaces.[14] Lamellar bodies used to be thought of as discrete granules that transport the contents from the Golgi apparatus to intercellular space. Recent evidence, however, has suggested a membrane folding model, in which the trans-Golgi network, lamellar bodes and intercellular space are all part of the same continuous membrane structure.[13,15] In this system, the synthesized molecules are easily released into the extracellular space through a cell surface pore via a continuous membrane-bound tube. Since the lamellar body was first found exclusively associated with the outer surface of the stratum granulosum, a lamellar body-related secretory system must be present to enable high concentration of HBD2 and HBD3 molecules to reach the outer layer of the epidermis and form a defensive barrier containing enough HBD2 and 3 to be effective.

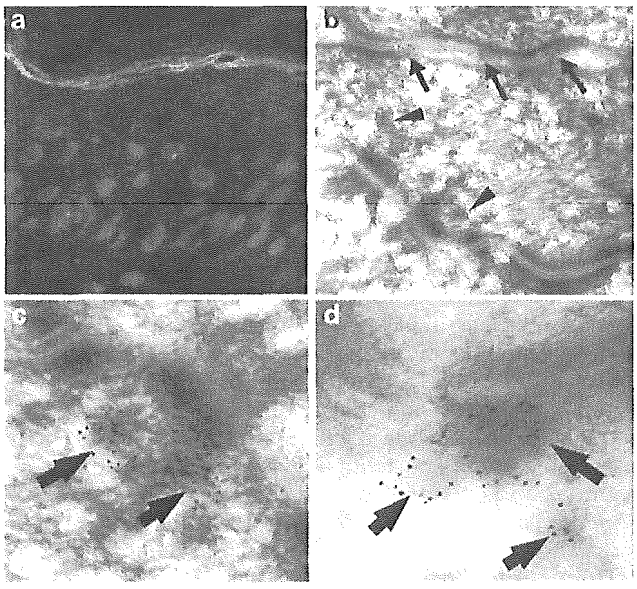

Figure 1 *(a) The localization of HBD3 was examined. Skin cryosections were cut from the biopsy skin specimens taken from normal volunteers and were incubated with the anti-human HBD3 rabbit polyclonal antibody (Novus Biologicals, Littleton, CO, USA). The second antibodies were goat anti-rabbit immunoglobulins conjugated to fluorescein (FITC). Immunostaining was detected as green (FITC) and the nuclear stain was observed as red (propidium iodide). HBD3 was located predominantly in the spinous and granular layers of the epidermis. (b–d) Immunoelectron microscopic analysis was performed. Normal skin samples were cryofixed with liquid propane cooled nitrogen, cryosubstituted at −80°C and low temperature embedded at −60°C in Lowicryl K11 M resin undergoing UV polymerization. Ultrathin sections were cut and immunogold stained using a 5 nm gold conjugated secondary (British Biocell, Cardiff, UK).[17] The anti-human HBD3 antibody and the anti-human cathepsin D rabbit polyclonal antibody (Santa Cruz Biotechnology, Santa Cruz, CA, USA) were used as primary antibodies and then a goat anti-rabbit IgG gold-conjugated secondary antibody (British Biocell, Cardiff, UK) was used. Gold particles were observed in the intercellular spaces of the stratum corneum (→) and in lamellar bodies of intracellular spaces (▼) often seen immediately beneath the apical plasma membrane of granular layer keratinocytes. Magnification: HDB3; (b) 25 000 ×, (c) 60 000 ×; cathepsin D; (d) 60 0000 ×.*

To establish a keratinocyte cell line that stably expresses HBD3, we first introduced the plasmid pFRT/lacZeo (Invitrogen, Carlsbad, CA, USA) into a human keratinocyte cell line, HaCaT cells, and subsequently prepared the Flp-In-HaCaT cells with the integrated Flp recombination target (FRT) site, which were also stably expressing β-galactosidase from the plasmid. Then, HBD3 cDNA was integrated into the FRT site already in the Flp-In-HaCaT cell genome, resulting in the establishment of an HBD3-HaCaT cell line. Immunostaining using anti-HBD3 antibodies showed that the cultured HBD3-HaCaT cell line expressed significant amounts of HBD3 (data not shown).

Our ultrastructural study showed that HBD3 was normally secreted though a special secretory system closely related to or identical with lamellar bodies *in vivo* (Figure 1). We then wondered whether this transgene synthesis and transfer from keratinocytes was released HBD3 into the culture medium. Before examining the culture medium, the activity of synthetic HBD3 was estimated using Gram-positive *S. aureus* strains ATCC6538 (AT), SA015 (SA-1) and SA092 (SA-2). Synthetic HBD3 showed almost the same antimicrobial activity against the three *S. aureus* strains (Figure 2a). It started to show killing activity in the microgram order and the concentration necessary to kill 50 % bacteria of SA-1 was approximately 8 μg/ml. Subsequently, colony-forming assays were performed to determine the antibacterial activity of HBD3-HaCaT cell culture medium. The apparent antimicrobial activity found from the 25 × concentrated sample and 50% killing activity was observed in the 100 × concentrated sample in SA-1 (Figure 2b). The supernatant of Fip-in-HaCaT cells as a control exhibited no killing activity against the bacteria. To determine the precise concentration of HBD3 in the culture medium, we performed immunodot blot analysis. The concentration of HBD3 in HBD3-HaCaT cell culture medium was 9.2 ng/ml (Figure 3c), while those of HaCaT and the Flp-In-HaCaT cells showed little or no detectable amount. Comparison with the result of synthetic HBD3 (Figure 2a) suggested that recombinant HBD3 from HaCaT cells had more antimicrobial activity than synthetic HBD3.

An epidermal sheet of HBD3-HaCaT cells was prepared and grafted onto an artificially induced ulcer in a nude rat (Figure 3a (1–3)). Immunohistochemical analysis using an anti-HBD3 antibody found strong reactivity in the graft, HBD3 engineered epidermis, while little or no reactivity was seen in the control epidermis of grafted Flp-In-HaCaT cells (Figure 3a (4,5)). The expression of HBD3 was stronger in the upper layers than the lower layers of the epidermis. On the other hand,

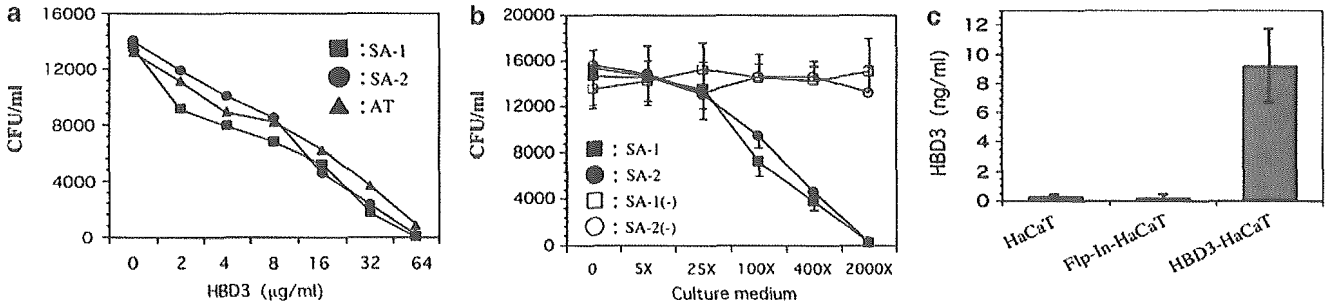

Figure 2 *(a) Peptide HBD3 was chemically synthesized according to the cDNA sequence.[5] Bacterial strains, Gram-positive S. aureus: ATCC6538 (AT), SA015 (SA-1) and SA092 (SA-2), used for experiments. SA-1 and SA-2 were isolated from patients with skin infection that was sensitive to antibiotics and kindly given by Fujisawa Pharmaceutical Co., Ltd, Osaka, Japan. The bacteria were incubated with synthetic HBD3 in 200 μl of 10 mM sodium phosphate buffer (pH 7.4) containing 1% trypticase soy broth for 3 h at 37°C. We measured the antimicrobial activity of HBD3 using the same media as used in the previous paper.[5] The antibiotic activity was estimated by plating serial dilutions of the incubation mixture and calculation of the colony-forming unit (CFU) after 24 h. (b) The human keratinocyte cell line HaCaT[18] was maintained in Dulbecco's modified Eagles's medium with 10% fetal bovine serum. Flp-In system (Invitrogen, Carlsbad, CA, USA) was utilized for generating stable expression cell line. In this system, Flp recombinase-mediated recombination occurs between specific Flp Recombination Target (FRT) sites. To integrate the FRT site into the genome of HaCaT cells, we first introduced plasmid pFRT/lacZeo and selected for Flp-In-HaCaT cells by medium containing zeocin. Fip-in-HaCaT cells expressed a lacZ-Zeocin fusion gene could be also detected by β-galactosidase staining. To amplify the coding regions of HBD3 cDNA by PCR, we synthesized two primer sets, 5'-TTTAAGCTTAGCAGCTATGAG GATCC-3' and 5'-GGGCTCGAGGGTTTTTATTTCTTTC-3' for the HBD3 cDNA. PCR was performed with oligo-(dT)-primed human keratinocyte cDNA as template. The PCR fragments were digested with restriction enzymes and subcloned into a multicloning site of plasmid pcDNA5/FRT, in which the inserted cDNA was driven by the CMV promoter. We performed co-transfection of the pcDNA5/FRT with HBD3 cDNA and the Flp recombinase expression vector pOG44. Finally, Flp-In-HaCaT cells with integration of HBD3 cDNA were selected by medium containing hygromycin. The cell line was referred as HBD3-HaCaT cell. The culture medium without antibiotics and fetal calf serum collected, treated with Centricon YM-3 Centrifugal Filter Unit (Millipore: Bedford, MA, USA) for concentration and desalting and subjected to colony-forming assay. Each value shown represents the mean ± s.d. of three individual samples. (● ■) HBD3-HaCaT cell, (○ □) Flp-In-HaCaT as control. (c) The concentration of HBD3 in the culture medium was determined by immunodot blot analysis.[16] Positive control and standard curve were generated with synthetic HBD3 peptides. Briefly, 5 μl of the concentrated medium (from the above samples) and serially diluted synthetic HBD3 were dotted in triplicate on nitrocellulose membrane. The membrane was incubated with the anti-human HBD3 rabbit polyclonal antibodies at 4°C overnight, and then reacted with goat anti-rabbit antibodies conjugated with peroxidase at room temperature for 2 h. The resultant dot complexes were processed for Phototope HRP Western Blot Detection System (Cell Signaling, Beverly, MA, USA) according to the manufacturer's protocol. The amount shown represents the mean ± s.d. of three individual samples.*

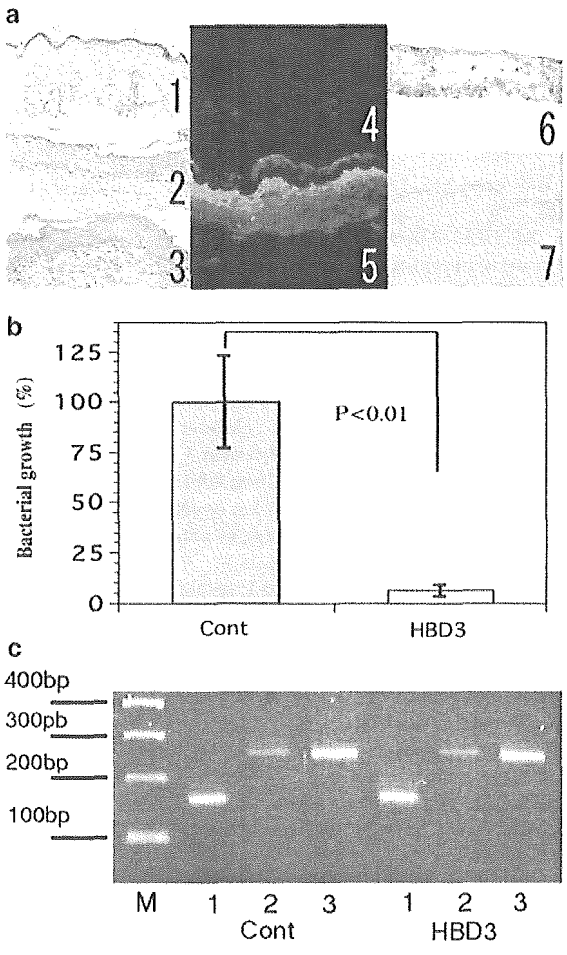

Figure 3 *(a) In nude rats (F344/N Jcl-rnu), the sites for transplantation were prepared by excising a 2 cm² area of dorsal epidermis and dermis. The confluent cultures of HBD3-HaCaT and control Flp-In-HaCaT were treated with dispase (1 nU/ml:Godo Shusei, Japan), and the floating epidermal sheet was placed on the prepared site of the nude rat. An occlusive dressing was quickly placed over the graft to hold it in position and to prevent it from drying. After 7 days, the skin sample was taken by excision. Afterwards, routine hematoxylin-eosin staining (1–3), immunostaining of the HBD3 antibody (4,5) and β-galactosidase staining (6,7) were performed. (1) normal rat; (2,4,6) the skin from Flp-In-HaCaT; (3,5,7) the skin from HBD3-HaCaT. (b) At 5 days after transplantation, the serial dilution of bacterial culture of SA-1 was applied to the graft and was overlaid with an occlusive dressing in wet condition. After 8 h incubation, the samples were collected from the surface of the graft with a sterile cotton swab, and transferred to the culture medium. The CFU was measured by plating. In each experiment, the CFU from the sample of HBD3-HaCaT was expressed as the rate against that of control Flp-In-HaCaT. Each group consisted of five rats and each value shown represents the mean ± s.d. of five individual samples. The student t-test detected a significant difference, $P < 0.01$; Cont versus HBD3. (c) We excised the rat epidermis surrounding both the control and HBD3 grafts. Epidermal sheets were obtained from the skin samples by treatment with 10 mg/ml dispase (3 h at 37°C).[19] Keratinocyte suspensions were obtained from these epidermal sheets by a further 0.25% trypsin treatment (30 min at 37°C). Total RNA was extracted from cultured cells and first strand cDNA was synthesized with reverse transcriptase (Life Sciences Inc., St Petersburg, FL, USA) using an oligo-dT primer. PCR was performed using following primers: 5'-GACACCAATCTCTACCGTCT-3' and 5'-ACCGGAAAGG CTGTATACCA-3' for rat CRAMP (GenBank accession no. AF484553); 5'-ATTTCTCCTGGTGCTGCTGT-3' and 5'-CTTGCAGCATCTCACTC TAG-3' for rat BD3 (NM 022544); 5'-AGCTGAACGGGAAGCTCACT-3' and 5'-CATTGAGAGCAATGCCAGCC-3' for rat GAPDH (NM 017008) as control. (M) 100 bp size marker, (1) BD3 (147 bp), (2) CRAMP (250 bp), (3) GAPDH: (246 bp).*

β-galactosidase staining showed strong activity in the control epidermis, but not in the HBD3 engineered epidermis (Figure 3a (6,7)). To ascertain the precise antimicrobial activity of the engineered skin, we applied bacteria SA-1 to the grafted epidermis and performed a colony-forming assay. The results demonstrated that significant antibacterial activity ($P<0.01$) was present in the HBD3 engineered epidermis compared with the control epidermis (Figure 3b). We examined the effect of the rat's endogenously produced antimicrobial peptides from the surrounding skin of the HBD3 and control grafts, but could not detect difference in expression of rat cathelicidine cathelin-related antimicrobial peptide (CRAMP) or BD3 (Figure 3c).

We demonstrated HBD3 killing activity in the culture medium; however, the HBD3 concentration in the supernatant was only 9.2 ng/ml, which was insufficient for significant antimicrobial activity. Therefore, we postulated that this HBD3 engineered epidermis might not show any significant antibacterial activity *in vivo*. However, our results showed that the HBD3 gene transfected epidermis formed an effective barrier that could withstand the attack of invading bacteria. These data suggested that the conditions *in vivo* might be a more suitable environment for keratinocytes to produce HBD3 and also utilize a more 'normal' lamellar body-related secretory system already in place for HBD3 in the appropriate position to prevent or protect from micro-organism attack.

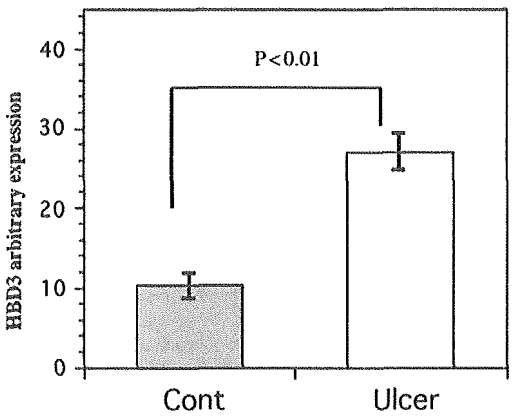

Figure 4 *The skin samples were collected from six patients with skin ulcer resulting from trauma and deep dermal burn during treatment at the Hokkaido University Hospital. Informed consent was obtained from individual subjects. We selected the patients with re-epithelizing ulcers at the healing stage, but the ulcer was so large that complete epithelization was expected to take a considerable time and to lead to hypertrophic scar formation. During operations we removed the skin samples from the ulcer with 0.5 cm margin. To prepare keratinocytes, we first separated the epidermis from dermis and subcutaneous tissue. Normal skin samples were obtained from seven patients undergoing reconstructive plastic surgery. Epidermal sheets were obtained from the skin samples by treatment with 10 mg/ml dispase (3 h at 37°C).[19] Keratinocyte suspensions were obtained from these epidermal sheets by a further 0.25% trypsin treatment (30 min at 37°C). Total RNA was extracted from cultured cells and first strand cDNA was synthesized with reverse transcriptase (Life Sciences Inc., St Petersburg, FL, USA) using an oligo-dT primer. Assays-on-Demand™ Products for HBD3 and GAPDH were purchased from Applied Biosystems (Foster City, CA, USA). The 50 μl reaction in each well contained 1 μl of total cDNA, 300 nm of sequence-specific primers and 200 nm of dual-labeled fluorogenic probe in 1 Taqman Universal PCR master mix (Applied Biosystems). A negative PCR control without template and a positive PCR control with a template of known amplification were included in each assay. The reaction was performed in an ABI PRISM 7700 Sequence Detection System. The HBD3 specific signal was normalized by constitutively expressed GAPDH and expressed as arbitrary scale. Ulcer: ulcer skin samples, Cont: normal skin samples. Each value indicated the mean±s.d. The student's t-test detected a significant difference, $P<0.01$; Cont versus Ulcer.*

One of the worst situations for preventing the tissue from bacterial invasion is in skin ulcers without any epidermal covering. If HBD3 plays a critical role in defending bacterial invasion in the skin, we hypothesized that re-epithelizing epidermis surrounding the ulcer wound might express a much higher level of HBD3. We therefore collected skin samples from patients with skin ulcers and examined the expression of HBD3 mRNA levels in the epidermis. As we expected, the epidermal samples in the ulcer skin expressed 2.5 times higher levels of HBD3 transcript than those in control skin (Figure 4). This result also suggested an increase in defensin expression as one of the major antimicrobial defense systems that can form an effective response to protect tissue from bacterial invasion.

Atopic dermatitis is a chronic inflammatory intractable skin disorder with unknown etiology. Atopic dermatitis skin lesions are often associated with higher than normal bacterial and viral infections, and atopic dermatitis skin has demonstrated a significant decrease expression of cathelicidin LL-37 and HBD2.[16] This evidence also led us to introduce the HBD3 gene into the epidermis and we have proved that the HBD3 gene transfected epidermis had a highly protective shield against bacterial invasion. The gene therapeutic introduction of HBD3 gene or the related genes into somatic cells may provide a new strategy for gene therapy for intractable infectious diseases.

References

1 Ganz T, Selsted ME, Lehrer RI. Defensins. *Eur J Haematol* 1990; **44**: 1–8.
2 Lehrer RI, Lichtenstein AK, Ganz T. Defensins: antimicrobial and cytotoxic peptides of mammalian cells. *Annu Rev Immunol* 1993; **11**: 105–128.
3 Bensch KW *et al*. hBD-1: a novel beta-defensin from human plasma. *FEBS Lett* 1995; **368**: 331–335.
4 Harder J, Bartels J, Christophers E, Schroder JM. A peptide antibiotic from human skin. *Nature* 1997; **387**: 861.
5 Harder J, Bartels J, Christophers E, Schroder JM. Isolation and characterization of human beta-defensin-3, a novel human inducible peptide antibiotic. *J Biol Chem* 2001; **276**: 5707–5713.
6 Garcia JR *et al*. Human beta-defensin 4: a novel inducible peptide with a specific salt-sensitive spectrum of antimicrobial activity. *FASEB J* 2001; **15**: 1819–1821.
7 Valore EV *et al*. Human beta-defensin-1: an antimicrobial peptide of urogenital tissues. *J Clin Invest* 1998; **101**: 1633–1642.
8 Harder J *et al*. Mucoid *Pseudomonas aeruginosa*, TNF-alpha, and IL-1beta, but not IL-6, induce human beta-defensin-2 in respiratory epithelia. *Am J Respir Cell Mol Biol* 2000; **22**: 714–721.
9 Bals R, Weiner DJ, Meegalla RL, Wilson JM. Transfer of a cathelicidin peptide antibiotic gene restores bacterial killing in a cystic fibrosis xenograft model. *J Clin Invest* 1999; **103**: 1113–1117.
10 Nikol S *et al*. Needle injection catheter delivery of the gene for an antibacterial agent inhibits neointimal formation. *Gene Therapy* 1999; **6**: 737–748.
11 Huang GT *et al*. A model for antimicrobial gene therapy: demonstration of human beta-defensin 2 antimicrobial activities *in vivo*. *Hum Gene Ther* 2002; **13**: 2017–2025.

12 Horikoshi T *et al.* Role of endogeneous cathepsin D-like and chymotrypsin-like proteolysis in human epidermal desquamation. *Br J Dermatol* 1999; **141**: 453–459.
13 Ishida-Yamamoto A *et al.* Epidermal lamellar granules transport different cargoes as distinct aggregates. *J Invest Dermatol* 2004; **122**: 1137–1144.
14 Oren A, Ganz T, Liu L, Meerloo T. In human epidermis, beta-defensin 2 is packaged in lamellar bodies. *Exp Mol Pathol* 2003; **74**: 180–182.
15 Norlen L. Skin barrier structure and function: the single gel phase model. *J Invest Dermatol* 2001; **117**: 830–836.
16 Fellermann K, Wehkamp J, Stange EF. Antimicrobial peptides in the skin. *N Engl J Med* 2003; **348**: 361–363.
17 Simizu H, McDonald JN, Kennedy AR, Eady RA. Demonstration of intra- and extracellular localization of bullous pemphigoid antigen using cryofixation and freeze substitution for embedding immunoelectron microscopy. *Arch Dermatol Res* 1989; **106**: 443–448.
18 Boukamp P *et al.* Normal keratinization in a spontaneously immortalized aneuploid human keratinocyte cell line. *J Cell Biol* 1988; **106**: 761–771.
19 Sawamura D *et al.* Induction of keratinocyte proliferation and lymphocytic infiltration by *in vivo* introduction of the IL-6 gene into keratinocytes and possibility of keratinocyte gene therapy for inflammatory skin diseases using IL-6 mutant genes. *J Immunol* 1998; **161**: 5633–5639.

Genes and Immunity (2005) 6, 285–289

www.nature.com/gene

FULL PAPER

Promoter region polymorphism of macrophage migration inhibitory factor is strong risk factor for young onset of extensive alopecia areata

T Shimizu[1], N Hizawa[2], A Honda[1], Y Zhao[1], R Abe[1], H Watanabe[1], J Nishihira[3], M Nishimura[2] and H Shimizu[1]

[1]*Department of Dermatology, Hokkaido University Graduate School of Medicine, Sapporo, Japan;* [2]*First Department of Medicine, Hokkaido University Graduate School of Medicine, Sapporo, Japan;* [3]*Genetic Laboratory, Sapporo, Japan*

*We have demonstrated that serum macrophage migration inhibitory factor (MIF) was significantly elevated in patients with extensive alopecia areata (AA). Recently, functional polymorphisms have been identified in the MIF promoter region. To address the functional and prognostic relevance of the −173G/C and −794[CATT]$_{5-8}$ repeat polymorphisms in MIF genes in patients with extensive AA, 113 patients with extensive AA and 194 healthy controls were genotyped. We found that MIF−173*C was a risk factor for early onset (<20 years) of extensive AA (odds ratio for GC heterozygotes with −173G/C was 4.88 (95% CI, 2.04–11.8), P=0.00038; odds ratio for CC homozygotes with −173G/C was 10.42 (95% CI, 2.56–43.5), P=0.0011). We found no statistically significant differences in the genotype frequencies of the −794[CATT]$_{5-8}$ repeat polymorphism and extensive AA. These results suggest that polymorphisms within the MIF−173*C allele confer an increased risk of susceptibility to the extensive forms of AA, especially with an early onset of disease. MIF is therefore suggested to be closely implicated in the pathogenesis of the more extensive forms of AA.*
Genes and Immunity (2005) **6,** 285–289. doi:10.1038/sj.gene.6364191
Published online 7 April 2005

Keywords: *macrophage migration inhibitory factor; alopecia areata; polymorphism; cytokine*

Introduction

The pathogenesis of alopecia areata (AA) is still uncertain. The immune system has been implicated in its pathogenesis and certain immunomodulatory cytokines may play an important role in this disease. The contribution of cytokines thought to be involved in the pathogenesis of AA has been well studied. Several lines of clinical and experimental data point toward cytokines such as interleukin (IL)-1 and tumor necrosis factor (TNF)-α, as being crucial inducers of hair loss in AA. The distribution of hair loss in patients with the TNF-α phenotype −308 was different between patients with the patchy form of disease and patients with alopecia totalis (AT) or alopecia universalis (AU) disease.[1] Recently, a strong association was reported between polymorphisms in the IL-1 receptor antagonist gene (IL1RN) at position +4734, IL1RN+2018 and AA.[2] In these studies, the presence of a genetic heterogeneity was suggested to account for the differences in disease severity and to influence the age of onset of AA.

Macrophage migration inhibitory factor (MIF) was the first lymphokine reported to prevent the random migration of macrophages.[3] A recent finding demonstrated that MIF functions as an initiator of inflammation and the immune response by regulation of a number of proinflammatory cytokines, including TNF-α and IL-1.[4] In human inflammatory diseases, MIF has a regulatory role in acute respiratory distress syndrome, asthma, rheumatoid arthritis and additionally in skin inflammatory diseases, such as atopic dermatitis.[5] Recently, functional polymorphisms have also been identified in the MIF promoter region; single nucleotide polymorphisms (SNPs) at position −173 (G to C) and in a tetranucleotide CATT repeat beginning at nucleotide position −794 have been associated with altered levels of MIF gene transcription *in vitro*.[6,7]

We previously reported that serum MIF is increased in patients with extensive AA and postulated that MIF might play a key role in the pathogenesis of extensive AA.[8] In the present study, we examined whether MIF gene promoter polymorphisms contribute to the risk of more extensive or early-onset forms of AA.

Correspondence: Dr T Shimizu, Department of Dermatology, Hokkaido University Graduate School of Medicine, Kita-ku, Kita-15, Nishi 7, Sapporo 060-8638, Japan. E-mail: michiki@med.hokudai.ac.jp
Received 11 January 2005; revised 14 February 2005; accepted 14 February 2005; published online 7 April 2005

Results

The distribution of MIF−173G/C and −794[CATT]$_{5-8}$ repeat polymorphisms in extensive AA and controls is

shown in Table 1. The genotype distribution for each polymorphism was in Hardy–Weinberg equilibrium in patients with extensive AA as well as in control subjects. None of the MIF−173G/C and −794[CATT]$_{5-8}$ promoter genotypes were associated with the development of extensive AA patients (Table 2). We also related these polymorphisms to subgroups of patients with AA stratified by disease severity or age of disease onset. A severity of alopecia tool (SALT) score was used to subdivide the severity of AA,[9] which were AA multiplex (SALT score S_3 and S_4) and AT/AU (SALT score S_5). We found that the MIF−173*C is a risk factor for disease early onset (<20 years); GG homozygotes odds ratio (OR) for GC heterozygotes of the −173G/C polymorphism was 4.88 (95% confidence interval (CI), 2.04–11.8; $P=0.00038$) and the OR for CC homozygotes of the −173G/C polymorphism was 10.42 (95% CI, 2.56–43.5; $P=0.0011$), calculated using the SYSTAT software (Table 2). Individuals with the GC or CC genotype had significantly higher risk for early age at onset of AA (<20 years); compared with GG homozygotes, odds ratio (OR) for GC genotype (OR, 5.5; 95% CI, 2.35–12.9; $P=0.00009$). Compared with the older onset of AA, the GC or CC genotype was also significantly frequent in the younger onset of the disease (OR, 30.3; 95% CI, 7.5–121.8; $P<0.00001$). In contrast, the −794[CATT]$_{5-8}$ repeat polymorphism was associated with none of the AA subgroups (Table 2).

Analysis using the haplo.em program showed that the −173G/C and −794[CATT]$_{5-8}$ promoter polymorphisms were in significant linkage disequilibrium with the −173C allele strongly associated with the 7-CATT repeat allele (the likelihood ratio statistic=217.8, df=2, $P<0.000001$). Haplotype analyses using the haplo.score program for early age at onset of AA (<20 years) revealed that the global score statistic was 64.102 (df= 6, $P<0.0001$, Global stimulation $P=0.0002$, based on 20 000 simulation repetitions) and the empirical P-value for the max-statistic was 0.0024 (Table 3). As judged by the haplotype-specific scores, the G/5-CATT haplotype was associated with a lower risk of AA ($P=0.0001$). On the other hand, C/5-CATT and C/7-CATT haplotypes were

Table 1 MIF−173G/C and 794 [CATT]$_{5-8}$ repeat polymorphism in extensive AA patients and controls[a]

	Controls (*n*=194)	*AA* (*n*=113)	*AA young* (*n*=55) *Age at onset <20 years*	*AA old* (*n*=58) *Age at onset ⩾20 years*	*AT/AU* (*n*=67)	*AA multiplex* (*n*=46)
−173G/C						
G/G	112 (57.8)	62 (54.9)	18 (32.7)	44 (75.9)	29 (43.3)	33 (71.7)
G/C	74 (38.1)	43 (38.0)	30 (54.6)	13 (22.4)	31 (46.3)	12 (26.1)
C/C	8 (4.1)	8 (7.1)	7 (12.7)	1 (1.7)	7 (10.4)	1 (2.2)
−794 [CATT]$_{5-8}$						
5,5	31 (16.0)	8 (7.1)	6 (10.9)	2 (3.4)	6 (9.0)	2 (4.3)
5,6	60 (30.9)	40 (35.4)	11 (20.0)	29 (50.0)	22 (32.8)	16 (39.1)
5,7	33 (17.0)	19 (16.8)	14 (25.5)	5 (8.6)	17 (25.4)	2 (4.3)
5,8	1 (0.5)	0 (0)	0 (0)	0 (0)	0 (0)	0 (0)
6,6	37 (19.1)	24 (21.2)	8 (14.5)	16 (27.6)	7 (10.4)	17 (37.0)
6,7	25 (12.9)	19 (16.8)	13 (23.6)	6 (10.4)	12 (17.9)	7 (15.3)
6,8	1 (0.5)	0 (0)	0 (0)	0 (0)	0 (0)	0 (0)
7,7	6 (3.1)	3 (2.7)	3 (5.5)	0 (0)	3 (4.5)	0 (0)

[a]Values are number (%).
AT: complete loss of all hair on the scalp; AU: complete loss of the entire body hair (SALT score S_5); AA multiplex patients can involve more than 50% hair loss of the scalp (SALT score S_3 and S_4).

Table 2 Impact of MI F−173G/C and −794 [CATT]$_{5-8}$ repeat polymorphisms on AA patients

	AA (n=113)		*AA young (n=55)*		*AA old (n=58)*		*AT/AU (n=67)*		*AA multiplex (n=46)*	
	OR (95% CI)	*P*	*OR (95% CI)*	*P*	*OR (95% CI)*	*P*	*OR (95% CI)*	*P*	*OR (95% CI)*	*P*
−173G/C										
GG	1	Ref	1	Ref	1	Ref	1	Ref	1	Ref
GC	1.03 (0.6, 1.75)	0.920	4.88 (2.04, 11.8)	0.00038*	0.41 (0.20, 0.84)	0.015	1.82 (0.93, 3.57)	0.08	0.55 (0.26, 1.16)	0.12
CC	1.61 (0.53, 4.89)	0.400	10.42 (2.56, 43.5)	0.0011*	0.25 (0.03, 2.17)	0.21	3.03 (0.89, 10.0)	0.07	0.34 (0.04, 2.94)	0.33
−794CATT										
55	1	Ref	1	Ref	1	Ref	1	Ref	1	Ref
5X	2.56 (1.02, 6.44)	0.046	1.43 (0.44, 4.55)	0.55	4.76 (1.10, 21.7)	0.041	2.52 (0.85, 7.40)	0.09	3.03 (0.65, 13.9)	0.160
XX	2.75 (1.10, 7.08)	0.036	2.91 (0.87, 10.0)	0.083	4.26 (0.92, 19.6)	0.064	2.14 (0.69, 6.60)	0.19	5.26 (1.12, 23.8)	0.036

AA: alopceia areata; OR: odds ratio; CI: confidence intervals.
The analysis of AA was adjusted for disease severity (AA multiplex and AT/AU) and early disease onset.
*$P<0.01$ after correction for multiple comparison.

Table 3 Frequencies of estimated CATT-MIF-173 haplotypes in extensive AA patients (age at onset <20 years)

Haplotype	*Hap-Freq (%)*	*Hap-Score*	*P-values (empirical)*
G/5-CATT	33.4	−3.81	0.0001
C/5-CATT	5.4	3.28	0.0019
G/6-CATT	37.9	−0.74	0.47
C/6-CATT	2.2	−0.62	0.56
G/7-CATT	1.8	1.07	0.30
C/7-CATT	18.9	3.24	0.0011
Total	100.0		

The analysis was adjusted for sex and age. Global statistic = 64.102, df = 6, $P < 0.0001$; global simulation $P = 0.0002$; max-statistic simulation $P = 0.0024$; number of simulations = 20 000.

associated with an increased risk of AA ($P = 0.0019$ and 0.0011, respectively) (Table 3). When the frequencies of the C/7-CATT haplotype and the other haplotypes combined were compared, higher frequency of the C/7-CATT haplotype was found in early age at onset of AA than that in controls ($\chi^2 = 5.17$, $P = 0.023$) or in older age at onset of the disease ($\chi^2 = 12.45$, $P = 0.00042$).

We then examined luciferase activity using the Dual-Luciferase Reporter Assay System, and found that transfection of the clone containing the C/7-CATT haplotypes into CEMC7 cells resulted in significantly increased luciferase activity relative to cells containing G/5-CATT haplotype ($P < 0.001$) (Figure 1).

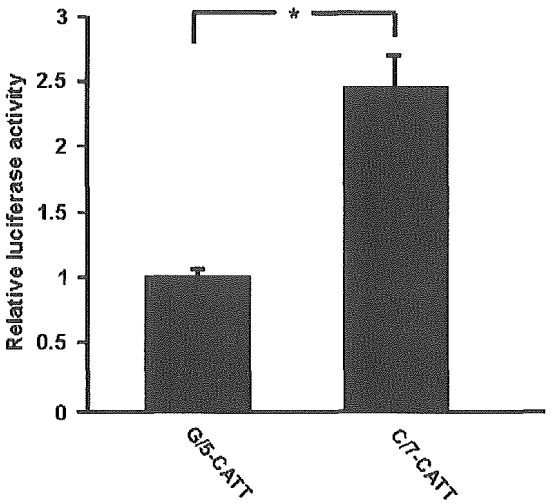

Figure 1 Analysis of MIF reporter activity. MIF promoter activity was determined by dual-luciferase assays, the results of which are expressed as relative luciferase activities. $N = 6$ number of replicates were examined, $^*P < 0.001$.

Discussion

In the present study, we have demonstrated that MIF−173*C is a risk factor for early onset extensive form of AA (<20 years). Furthermore, the MIF−C/7-CATT haplotype was closely associated with an increased risk of extensive AA in early-onset patients. Transfection of the clone containing the C/7-CATT haplotype into a T-lymphoblast cell line resulted in significantly increased luciferase activity compared to that of G/5-CATT haplotype, supporting these findings. MIF was originally identified as a lymphokine that concentrates macrophages at inflammatory loci, is a potent activator of macrophages *in vivo* and is considered to play an important role in cell-mediated immunity.[3,10] Since the molecular cloning of MIF,[11] this cytokine has been re-evaluated as a proinflammatory cytokine and pituitary-derived hormone that potentiates endotoxemia.[12,13] It has been shown that T cells and macrophages secrete MIF in response to various proinflammatory stimuli such as endotoxins.[4]

It is evident that the mechanisms of hair follicle dysfunction in AA are immunological and controlled by activated T cells.[14] Hair loss is associated with a perifollicular lymphocytic infiltrate made up primarily of CD4+ cells, along with a CD8+ intrafollicular infiltrate. Although the function of these T cells in disease pathogenesis is not fully understood, cytokines released from T cells seem to be important mediators leading to AA hair loss. Proinflammatory cytokines lead to reductions in growth factor secretion by dermal papilla fibroblasts and result in premature catagen stage development, which is characterized by an abnormal pattern of cell degeneration and apoptosis.[15] IL-1 and TNF-α may play a particular role in the AA pathophysiology of inflammatory hair loss. IL-1 has been shown to inhibit hair growth *in vitro* and may be one of the factors triggering the arrest of hair growth *in vivo*.[16] TNF-α also inhibits hair follicle growth *in vitro*.[17] The IL-1 and TNF-α gene polymorphisms have been previously investigated. Galbraith *et al*[18] found evidence of increased susceptibility to AA with certain IL-1/immunoglobulin κ light-chain genotypes. The association has been reported between the severity of AA and the inheritance of allele 2 of a five-allele variable number tandem repeat polymorphism in intron 2 of the IL1RN.[19] A stronger association with IL1RN was observed in patients with severe AA and in those with early-onset disease (<20 years).[2] A TNF-α polymorphism was also studied in AA and a significant difference was found in TNF-308 genotype between patients with patchy disease and those with AT/AU.[1] These previous studies strongly suggested the presence of genetic heterogeneity in the more extensive forms of AA.

It was speculated that MIF may be produced by multiple cellular sources in inflammatory and autoimmune diseases such as activated T lymphocytes and monocytes.[20,21] We have previously demonstrated that serum MIF was elevated in patients with extensive AA, and immunohistochemical MIF staining was positive for perifollicular-infiltrated lymphocytes in telogen hair follicles in patients with extensive AA.[8] On the basis of our results, we speculate that activated T cells might be a potential source of serum MIF. MIF levels may reflect the inflammatory symptoms in extensive AA. The direct pathogenic mechanism of MIF in AA is still unclear. Recently, the growth-inhibiting effects induced on fibroblasts by MIF has been reported.[22] Imbalance between proinflammatory cytokines and cytokine antagonists or inhibitors is one of the factors that may predispose patients to the initiation or perpetuation of autoimmune diseases including AA. It is known that the proinflammatory mediators IL-1 and TNF-α are potent

inhibitors of hair follicle cell proliferation, with a concomitant inhibition of hair growth.[17] MIF is upregulated by TNF-α, and MIF in turn augments the secretion TNF-α.[4,23] Therefore, these inflammatory cytokines may be implicated in the induction or continuation of damage to hair follicles, and MIF may play an important part in the pathophysiology of inflammatory hair loss as in AA.

The MIF gene maps to chromosome 22q11.2, and an SNP (G to C transition) in the 5′-flanking region at position 173 of the MIF gene is associated with susceptibility to adult inflammatory arthritis.[24] Donn *et al*[25,26] initially reported that individuals possessing the C allele had an increased risk of systemic-onset juvenile idiopathic arthritis (JIA), and later, that the MIF−173*C-CATT7 haplotype was associated with all JIA independent of subgroup. This polymorphism also has the potential to be associated with an increased expression of MIF via production of an activator protein-4 response element in the MIF promoter. A CATT tetranucleotide repeat element beginning at −794, within the MIF promoter, also appears to play a role in determining susceptibility to rheumatoid arthritis.[26] Recently, both MIF−173G/C and −794[CATT]$_{5-8}$ repeat polymorphisms in the MIF promoter region have been associated with altered levels of MIF gene transcription, and significant association between the −173G/C and −794[CATT]$_{5-8}$ repeat polymorphisms and atopy in a sample of the Japanese population was found.[27] In inflammatory skin diseases, the presence of the MIF−173*C polymorphism or the −794[CATT]$_{5-8}$ repeat polymorphism was positively correlated with psoriasis in Caucasian patients.[26]

Our findings support evidence that polymorphisms in the MIF−173*C allele confer an increased risk of susceptibility to the more severe or extensive forms of AA in the Japanese population, especially in early-onset disease subtypes. Since these cytokine-related alleles are clearly associated with AA, our present study further implicates a vital role of MIF in the pathogenesis of AA.

Materials and methods

Patients and controls

SALT scores were used to subdivide the severity of AA, and we defined more than 50% hair loss of the scalp (SALT score S_3–S_5) as extensive AA in this study.[9] Peripheral blood samples were obtained, with informed consent, from 113 Japanese patients with extensive AA recruited from dermatology clinics in Hokkaido University, Sapporo, Japan. The age range was 5–76 years (mean 32.2) and included 40 male and 73 female subjects. All subjects gave written, informed consent for enrollment in the study and all associated procedures. The Ethics Committee of the Hokkaido University School of Medicine approved this study. AA multiplex patients can involve more than 50% hair loss of the scalp (SALT score, S_3 and S_4). Six ophiasis type AA patients were included in this group. In more severe disease cases, the alopecia can progress to complete loss of all hair on the scalp, AT, or further to cause a complete loss of all body hair, AU (SALT score, S_5). Clinical information was updated at follow-up examinations. No family history of extensive AA (SALT score, S_3–S_5) was observed. We also divided the AA patients into two subgroups on the basis of age of disease onset, as previously described.[28] DNA samples from healthy controls were also obtained from 194 consecutive blood samples (aged 18–72 years, mean age 41.6 years; 115 male and 79 female subjects). Concomitant autoimmune diseases including thyroid diseases, and atopic dermatitis patients diagnosed according to the criteria of Hanifin and Rajika[29] were excluded in this study.

Screening for MIF polymorphism

For each individual, we genotyped the −173G/C promoter polymorphisms using the assay that combines kinetic (real-time quantitative) polymerase chain reaction (PCR) with allele-specific amplification in which primers were designed[30] (Primer Express software; PE Applied Biosystems, Foster City, CA, USA) to specifically amplify either the −173G or −173C allele in separate PCRs (−173G forward primer, 5′-CCGCCAAGTGGAGAA-CAGG-3′; −173C forward primer, 5′-CCGCCAAGTGGA GAACAGC 3′; −173G reverse primer, 5′-GGCGCACCG CTCCAAC-3′; −173C reverse primer, 5′-GGCGCACCGC TCCAAG-3′). The PCR products were detected using the ABI 7700 Sequence Detection System with a dsDNA-specific fluorescent dye SYBR Green I (PE Applied Biosystems). For typing of the CATT tetranucleotide repeat polymorphism beginning at −794, DNA was amplified by PCR using a carboxyfluorescein-labeled reverse primer (forward primer, 5′-TGCAGGAACCAA TACCCATAGG-3′; reverse primer, 5′-AATGG TAAACTCGGGGAC-3′). The PCR products were separated by electrophoresis through a performance-optimized polymer-4 gel using an ABI 310 DNA sequencer (PE Applied Biosystems). For each individual, allele sizes were calculated using the Genescan Analysis computer program (PE Applied Biosystems).

Luciferase reporter gene assay

Two plasmids were constructed, corresponding to the three prevalent haplotypes: G/5-CATT and C/7-CATT as previously described.[27] The human T-lymphoblast cell line, CEMC7 cell, was obtained from the Health Science Research Resources Bank (Osaka, Japan). CEMC7 cells (1×10^5) were then transfected with 0.1 μg of one of the three constructs and 0.1 μg of pRL-TK vector, an internal control for monitoring transfection efficiency. After 24 h, we measured luciferase activity using the Dual-Luciferase Reporter Assay System (Promega, Tokyo, Japan).

Statistical analysis

The association of MIF promoter polymorphisms was measured using an OR with 95% CI, as estimates of relative risk for development of AA. The −794[CATT]$_{5-8}$ genotypes were combined into three categories: 5, 5 genotype; 5, X genotypes; and X, X genotypes (allele X represents any allele other than five repeats of CATT). ORs were adjusted for sex and age. These analyses were conducted using the SYSTAT program (SPSS Inc.). We used the Hardy–Weinberg equilibrium program to compare observed numbers of genotypes with the numbers of genotypes expected under the normal Hardy–Weinberg equilibrium.[31] To evaluate linkage disequilibrium between −173G/C and −794CATT repeat polymorphisms, we used the haplo.em function in the Haplo.Stats program, which calculated the likelihood ratio statistic for linkage equilibrium by estimating haplotype frequencies. Haplotype analysis was conducted

using the haplo.score function in the Haplo.Stats program to test statistical association between the MIF haplotypes and AA, which performed adjustment for covariates and computation of simulation *P*-values for each haplotype.[32] All reporter gene data points were represented as the mean ± s.e.m. results of multiple, independent experiments. Differences were tested by the Student's *t*-test and were considered statistically significant at $P < 0.05$.

Acknowledgements

This research was supported by a Grant-in-Aid for research (nos. 11670813 and 13357008) from the Ministry of Education, Science, and Culture of Japan. We thank Dr James R McMillan for the proofreading of this manuscript.

References

1 Galbraith GM, Pandey JP. Tumor necrosis factor alpha (TNF-alpha) gene polymorphism in alopecia areata. *Hum Genet* 1995; **96**: 433–436.
2 Tazi-Ahnini R, Cox A, McDonagh AJ *et al*. Genetic analysis of the interleukin-1 receptor antagonist and its homologue IL-1L1 in alopecia areata: strong severity association and possible gene interaction. *Eur J Immunogenet* 2002; **29**: 25–30.
3 Bloom BR, Bennett B. Mechanism of reaction *in vivo* associated with delayed-type hypersensitivity. *Science* 1966; **153**: 80–82.
4 Calandra T, Bernhagen J, Mitchell RA, Bucala R. The macrophage is an important and previously unrecognized source of macrophage migration inhibitory factor. *J Exp Med* 1994; **179**: 1895–1902.
5 Shimizu T. Role of macrophage migration inhibitory factor (MIF) in the skin. *J Dermatol Sci* 2005; **37**: 65–73.
6 Donn R, Alourfi Z, De Benedetti F, *et al*, British Paediatric Rheumatology Study Group. Mutation screening of the macrophage migration inhibitory factor gene: positive association of a functional polymorphism of macrophage migration inhibitory factor with juvenile idiopathic arthritis. *Arthritis Rheum* 2002; **46**: 2402–2409.
7 Baugh JA, Chitnis S, Donnelly SC *et al*. A functional promoter polymorphism in the macrophage migration inhibitory factor (MIF) gene associated with disease severity in rheumatoid arthritis. *Genes Immun* 2002; **3**: 170–176.
8 Shimizu T, Nishihira J, Mizue Y, Abe R, Watanabe H, Shimizu H. Increased macrophage migration inhibitory factor (MIF) in sera of patients with extensive alopecia areata. *J Invest Dermatol* 2002; **118**: 555–557.
9 Olsen EA, Hordinsky MK, Price VH *et al*. Alopecia areata investigational assessment guidelines—Part II. *J Am Acad Dermatol* 2004; **51**: 440–447.
10 David JR. Delayed hypersensitivity *in vitro*: its mediation by cell-free substances formed by lymphoid cell–antigen interaction. *Proc Natl Acad Sci USA* 1966; **56**: 72–77.
11 Weiser WY, Temple PA, Witek-Giannotti JS, Remold HG, Clark SC, David JR. Molecular cloning of a cDNA encoding a human macrophage migration inhibitory factor. *Proc Natl Acad Sci USA* 1989; **86**: 7522–7526.
12 Bernhagen J, Calandra T, Mitchell RA *et al*. MIF is a pituitary-derived cytokine that potentiates lethal endotoxaemia. *Nature* 1993; **365**: 756–759.
13 Bucala R. MIF re-evaluated: pituitary hormone and glucocorticoid-induced regulator of cytokine production. *FASEB J* 1996; **7**: 19–24.
14 McDonagh AJ, Tazi-Ahnini R. Epidemiology and genetics of alopecia areata. Review. *Clin Exp Dermatol* 2002; **27**: 405–409.
15 Tobin SJ. Morphological analysis of hair follicles in alopecia areata. *Microsc Res Tech* 1997; **38**: 443–451.
16 Harmon CS, Nevins TD. IL-1α inhibits human hair follicle growth and hair fiber production in whole-organ cultures. *Lymphokines Cytokines Res* 1993; **12**: 197–203.
17 Philpott MP, Sanders DA, Bowen J, Kealey T. Effects of interleukins, colony-stimulating factor and tumour necrosis factor on human hair follicle growth *in vitro*: a possible role for interleukin-1 and tumour necrosis factor-alpha in alopecia areata. *Br J Dermatol* 1996; **135**: 942–948.
18 Galbraith GM, Palesch Y, Gore EA, Pandey JP. Contribution of interleukin 1beta and KM loci to alopecia areata. *Hum Hered* 1999; **49**: 85–89.
19 Tarlow JK, Clay FE, Cork MJ *et al*. Severity of alopecia areata is associated with a polymorphism in the interleukin-1 receptor antagonist gene. *J Invest Dermatol* 1994; **103**: 387–390.
20 Shimizu T, Abe R, Ohkawara A, Nishihira J. Increased production of macrophage migration inhibitory factor by PBMCs of atopic dermatitis. *J Allergy Clin Immunol* 1999; **104**: 659–664.
21 Foote A, Kipen Y, Santos L, Leech M, Morand EF. Macrophage migration inhibitory factor in systemic lupus erythematosus. *J Rheumatol* 2004; **31**: 268–273.
22 Kleemann R, Hausser A, Geiger G *et al*. Intracellular action of the cytokine MIF to modulate AP-1 activity and the cell cycle through Jab1. *Nature* 2000; **408**: 211–216.
23 Donnelly SC, Haslett C, Reid PT *et al*. Regulatory role for macrophage migration inhibitory factor in acute respiratory distress syndrome. *Nat Med* 1997; **3**: 320–323.
24 Barton A, Lamb R, Symmons D *et al*. Macrophage migration inhibitory factor (MIF) gene polymorphism is associated with susceptibility to but not severity of inflammatory polyarthritis. *Genes Immun* 2003; **4**: 487–491.
25 Donn RP, Shelley E, Oliver WE, Thomson W. A novel 5′-flanking region polymorphism of macrophage migration inhibitory factor is associated with systemic-onset juvenile idiopathic arthritis. *Arthritis Rheum* 2001; **44**: 1782–1785.
26 Donn R, Alourfi Z, Zeggini E, *et al*. British Paediatric Rheumatology Study Group. A functional promoter haplotype of macrophage migration inhibitory factor is linked and associated with juvenile idiopathic arthritis. *Arthritis Rheum* 2004; **50**: 1604–1610.
27 Hizawa N, Yamaguchi E, Takahashi D, Nishihira J, Nishimura M. Functional polymorphisms in the promoter region of macrophage migration inhibitory factor and atopy. *Am J Respir Crit Care Med* 2004; **169**: 1014–1018.
28 Colombe BW, Lou CD, Price VH. The genetic basis of alopecia areata: HLA associations with patchy alopecia areata *versus* alopecia totalis and alopecia universalis. *J Invest Dermatol Symp Proc* 1999; **4**: 216–219.
29 Hanifin JM, Rajika G. Diagnostic features of atopic dermatitis. *Acta Derm Venerol (Stockh)* 1980; **92** (Suppl): 44–47.
30 Germer S, Holland MJ, Higuchi R. High-throughput SNP allele-frequency determination in pooled DNA samples by kinetic PCR. *Genome Res* 2000; **10**: 258–266.
31 Terwillinger JD, Ott J. *Handbook of Human Genetic Linkage*. Johns Hopkins University Press, Baltimore, MD, 1994.
32 Schaid DJ, Rowland CM, Tines DE, Jacobson RM, Poland GA. Score tests for association between traits and haplotypes when linkage phase is ambiguous. *Am J Hum Genet* 2002; **70**: 425–434.

Experimental Dermatology 2005: 14: 819–823
Blackwell Munksgaard . Printed in Singapore

EXPERIMENTAL DERMATOLOGY
ISSN 0906-6705

Expression of macrophage migration inhibitory factor in rat skin during embryonic development

Shimizu T, Ogata A, Honda A, Nishihira J, Watanabe H, Abe R, Zhao Y, Shimizu H. Expression of macrophage migration inhibitory factor in rat skin during embryonic development.
Exp Dermatol 2005: 14: 819–823. © Blackwell Munksgaard, 2005

Abstract: We have previously shown that human epidermal keratinocytes express macrophage migration inhibitory factor (MIF) mRNA, and immunohistochemical studies showed that MIF is expressed in human epidermis. To explore the possible pathophysiological roles of MIF in skin during rat fetal development, we examined the expression patterns of MIF during rat epidermal development using Northern blot analysis and *in situ* hybridization. Expression of MIF mRNA was first detected by *in situ* hybridization in the developing epidermis and hair germ cells from embryonic day (ED) 16. From ED 19, moderate levels of MIF expression were detected in the epidermis and epithelial sheath cells of growing hair follicles. In postnatal rat skin, higher MIF expression was detected in the epidermis and hair follicles on postnatal day 3. These observations were also confirmed by Northern blot analysis. Immunohistochemical analysis with an anti-MIF antibody showed a similar distribution to that of the mRNA. Our results suggest that MIF is associated with epidermal and hair follicle development.

Tadamichi Shimizu[1], Akihiko Ogata[2], Ayumi Honda[1], Jun Nishihira[3], Hirokazu Watanabe[1], Riichiro Abe[1], Yunan Zhao[1] and Hiroshi Shimizu[1]

[1]Department of Dermatology, Hokkaido University Graduate School of Medicine, Sapporo, Japan;
[2]Department of Neurology, Hokkaido University Graduate School of Medicine, Sapporo, Japan;
[3]GeneticLab Co., Ltd. Sapporo, Japan

Key words: development – *in situ* hybridization – macrophage migration inhibitory factor – rat

Tadamichi Shimizu
Departments of Dermatology
Hokkaido University Graduate School of Medicine
Sapporo 060-8638
Japan
Tel.: +81 11 716 1161x5962
Fax: +81 11 706 7820
e-mail: michiki@med.hokudai.ac.jp

Accepted for publication 13 July 2005

Introduction

Macrophage migration inhibitory factor (MIF), which was originally identified as a lymphokine attractant for macrophages at inflammatory loci, is a potent activator of macrophages and is thought to play an important role in cell-mediated immunity (1). MIF was reportedly mainly expressed in T lymphocytes and macrophages; however, current studies revealed that this protein is ubiquitously expressed in various cells (2,3). Recently, it was reported that endotoxin treatment affects the expression of MIF protein and mRNA in various rat tissues (4). To date, MIF responses to stimuli such as wounding and infection are thought to contribute to the regulation of inflammatory and immunological tissue repair (1,4). In a previous study, we have shown using reverse transcription-polymerase chain reaction analysis that human epidermal keratinocytes express MIF mRNA, and our immunohistochemical studies showed that MIF is expressed in the human epidermis, especially within the basal layer (5). Although the pathophysiological function(s) of MIF in skin remains ambiguous, the fact that MIF is produced by keratinocytes points to a likely biological relevance in cutaneous inflammatory responses and cell growth and differentiation. To explore the possible pathophysiological roles of MIF in skin, we have examined the expression of MIF mRNA during rat fetal development using Northern blot analysis and *in situ* hybridization.

Abbreviations: ED, embryonic days; MIF, macrophage migration inhibitory factor; PD, postnatal days.

Materials and methods

Animals

Fischer rats, used in this study, were purchased from Nippon Clea (Shizuoka, Japan). Embryos were obtained from

pregnant rats at embryonic days (ED) 13, 16, and 19. They were rinsed briefly with 4% paraformaldehyde in 0.1 M phosphate buffer (PB) (pH 7.4) and fixed in the same solution at 4°C overnight. In addition, postnatal day (PD) 3 rats were used. Under ether anesthesia, they were perfused with 4% paraformaldehyde in 0.1 M PB (pH 7.4) and then fixed with solution at 4°C overnight.

Northern blot analysis

Total cellular RNA was isolated from the skin (epidermis plus dermis) of rats at ED 16, 19, and PD 3 using an Isogen extraction kit (Nippon Gene, Toyama, Japan) according to the manufacturer's protocols. Northern blot analysis was carried out as previously described (6). In brief, RNA (20 mg) was separated by electrophoresis on agarose gels containing 0.6 M formaldehyde and blotted onto nylon membrane filters. Hybridization was carried out with a rat MIF cDNA probe, radiolabeled with [α-^{32}P]dCTP by use of a random primer labeling kit. The hybridization was performed in a solution containing the radiolabeled rat MIF cDNA probe, 50% formamide, 0.75 M NaCl, 0.1% sodium dodecyl sulfate (SDS), 20 mM Tris-HCl (pH 7.5), 2.5 mM ethylenediaminetetraacetic acid (EDTA), 0.5× Denhardt's solution (1× Denhardt's solution: 2.5 mM EDTA, 0.5× albumin, 0.2% polyvinylpyrolidone, 0.2% Ficoll), and 10% dextran sulfate at 42°C overnight. After hybridization, the filters were washed with 0.2× standard saline citrate (SSC) (1× SSC: 0.15 M NaCl, 0.015 M sodium citrate), 0.1% SDS at 65°C and subjected to autoradiographic analysis. As a control, the filters were probed with radiolabeled glyceraldehyde-3-phosphate dehydrogenase (GAPDH). Hybridization signals were digitized and quantified with MCID Image Analyzer (Fuji Film, Tokyo, Japan). The density of MIF bands was normalized by the intensities of GAPDH.

In situ hybridization

A Digoxigenin (DIG)-labeled RNA probe complementary to the rat MIF mRNA was prepared using DIG RNA labeling kit (Boehringer Mannheim, St. Louis, MO, USA) as previously described (7). To prepare the template DNA for the rat MIF probe, the full-length sequence was subcloned into pBluescript SK(–) plasmid. This plasmid was either linearized with EcoRI and transcribed with T7 RNA polymerase to prepare an antisense probe or linearized with Hind III and transcribed with T3 RNA polymerase to prepare a sense probe. Using this probe, hybridization was carried out as previously described by Hirota et al. (8). In brief, slides (the skin of rats at ED 13, 16, 19, and PD 3) were hydrated and digested with 10 μg/ml protease K (Sigma, Tokyo, Japan) after deparaffinization. They were fixed with 4% paraformaldehyde in 0.1 M PB. Then, they were treated with 0.2 M HCl to inactivate endogenous alkaline phosphatase and were acetylated by 0.25% acetic anhydride in 0.1 M triethanolamine (pH 8.0). Following dehydration under air, they were incubated in hybridization buffer at 50°C overnight in a moistened chamber. The hybridization solution contained 50% deionized formamide, 10 mM Tris-HCl (pH 7.6), 200 μg/ml tRNA, 1× Denhardt's solution, 10% dextran sulfate, 600 mM NaCl, 1 mM EDTA pH 8.0, and 1 μg/ml of the RNA probe. Following this, slides were washed with 5× SSC(1× SSC: 0.15 M NaCl, 0.015 M sodium citrate) and then with 2× SSC, 50% formamide at 50°C. After the treatment with RNase A, the sections were blocked with a 1% blocking reagent (Boehringer Mannheim) and treated with anti-DIG antibody conjugated with alkaline phosphatase diluted to 1:500 (Boehringer Mannheim) at room temperature for 1 h. Nitroblue tetrazolium chloride and 5-bromo-4chloro-3-indolyl phosphate were used to visualize any positive signal. As a negative control, hybridization was also performed using a sense probe.

Immunohistochemistry

A polyclonal anti-rat MIF antibody was generated by immunizing New Zealand white rabbits with purified recombinant rat MIF as described previously (6). Rat skin of 13, 16, and 19 ED, and PD 3 was embedded in Tissue-Tek OCT Compound and snap frozen in liquid nitrogen and stored at –80°C. The frozen, embedded tissues were cut into 4-μm sections which were collected to slides and fixed in acetone for 10 min at room temperature. They were stained using an avidin–biotin peroxidase complex procedure using a Vector ABC Kit according to the manufacturer's protocol. In brief, the sections were incubated overnight at 4°C with the anti-rat MIF antibody (1:500 dilution). After three washes with phosphate-buffered saline (PBS), the samples were treated with biotinylated goat anti-rabbit immunoglobulin G (IgG) (Cell Signaling Technology, Inc., Beverly, MA, USA)(10 μg/ml) in PBS containing 1% bovine serum albumin and 0.05% NaN_3 for 30 min at 37°C. The slides were washed three times with PBS and were incubated with peroxidase-conjugated streptavidin (100 μg/ml) in PBS at room temperature for 30 min. The reaction was developed in 3,3′-diaminobenzidine tetrahydrochloride containing hydrogen peroxide (0.01%), and the tissue samples were mounted in alkylacrylate. Non-immune rabbit IgG was used as a negative control.

Results

Mild expression of MIF mRNA was first detected at ED 16 in the developing epidermis and developing hair germs (Fig. 1a). Mesenchymal cells in the dermis also expressed MIF mRNA. ED 13 samples failed to show MIF mRNA expression in the developing epidermis (data not shown). From ED 19 onwards, moderate MIF mRNA-expression levels were detected in the developing epidermis and epithelial hair follicle sheath cells (Fig. 1b,c). Sense RNA probes (negative control) showed no MIF mRNA expression in the epidermis (Fig. 1d). Immunohistochemical analysis with anti-MIF antibody at ED 13 failed to show staining in developing skin (data not shown). At ED 16, the anti-MIF antibody showed weak staining in the developing epidermis (Fig. 1e) and moderate staining in the epidermis and hair follicles at ED 19 (Fig. 1f). Non-immune IgG (negative control) failed to show any skin staining at ED 19 (Fig. 1g). In rat skin at PD 3, high expression of MIF mRNA was detected in the epidermis (Fig. 2a), and consistent expression was detected in the hair follicles (Fig. 3b). Immunohistochemical analysis with anti-MIF antibody at PD 3 showed a similar distribution to that seen in the *in situ* hybridization analysis (Fig. 2c). Northern blot analysis showed that MIF mRNA could be faintly detected in ED 16 skin (Fig. 3). MIF mRNA was up-regulated by ED 19 and was clearly detected in PD 3 skin (Fig. 3). Table 1 summarizes the MIF mRNA expression patterns in developing rat skin.

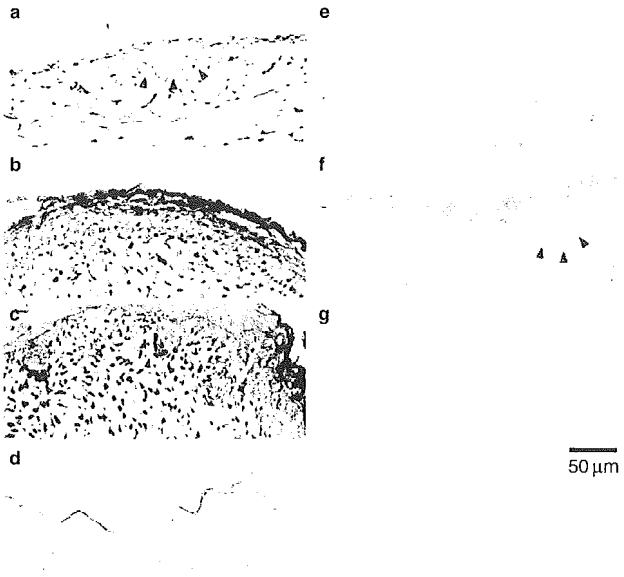

Figure 1. Expression of macrophage migration inhibitory factor (MIF) mRNA and protein in the embryonic stage. *In situ* hybridization using Digoxigenin (DIG)-labeled antisense MIF RNA probe on rat embryo skin sections. On embryonic day (ED) 16, MIF mRNA was first detected in the developing epidermis and hair germs (arrow head) (a). Mesenchymal cells in the dermis also expressed MIF mRNA. On ED 19, the mRNA signal was moderate in both the epidermis (b) and the hair follicles (arrow head) (c). Negative control sections incubated with the DIG-labeled sense MIF RNA probe failed to show any staining in skin at ED 19 (d). An immunohistochemical study using ED 16 rat skin with the anti-MIF polyclonal antibody showed less MIF staining in the developing epidermis (e). At ED 19, MIF was moderately stained in the epidermis and hair follicles (arrow head) (f). Non-immune immunoglobulin G showed no skin staining at ED 19 (g). Bar = 50 µm.

Discussion

MIF was the first lymphokine reported to prevent the random migration of macrophages and recruit them to inflammatory loci (9). MIF has long been considered as exclusively expressed in activated T lymphocytes; however, it is now clear that a variety of cells and tissues have the potential to produce this immunoregulatory protein. From these findings, novel immunological and hormonal MIF functions have been reported including those in the skin (10). Bernhagen et al. (11) reported that the administration of neutralizing anti-MIF antibodies in mice significantly inhibited the development of delayed-type hypersensitivity reactions, affirming the central role of MIF in the immunological response. MIF also counteracts the anti-inflammatory actions of the glucocorticoids (12) and plays an essential role in T-cell activation (13). Recently, we have identified the involvement of MIF in cutaneous wound healing (14,15). We found that MIF is critical for cutaneous inflammatory reactions and immune responses in the defense against ultraviolet B exposure (16). The two MIF-related protein of the S100 family are also expressed in epithelial cells under inflammatory conditions (17). These findings together suggest that MIF plays a critical role in skin inflammation and immunity.

The present study is the first report describing the expression of MIF during skin development. It is known that the epidermis is simple in its structure before ED 13.5 in the rat and that the embryonic epidermis becomes stratified after ED 16 (18). MIF mRNA expression was first detected in the developing epidermis at ED 16, indicating that MIF may be important for epidermal development. High MIF mRNA-expression levels were also detected in mesenchymal cells in the dermis at ED 16 and 19. It has been reported that ED 16 mesenchymal cells are able to induce greater numbers of hair bulbs than ED 14

Figure 2. Expression of macrophage migration inhibitory factor (MIF) mRNA and protein in postnatal rat skin. At postnatal day (PD) 3, MIF mRNA signal was strikingly expressed in the epidermis of the skin (a). The MIF mRNA signals were also highly expressed in hair follicles (arrow head) (b). An immunohistochemical study using PD 3 rat skin with the anti-MIF polyclonal antibody showed a similar distribution in the epidermis to that of the *in situ* hybridization (arrow indicate the epidermal basal layer) (c). Bar = 50 µm.

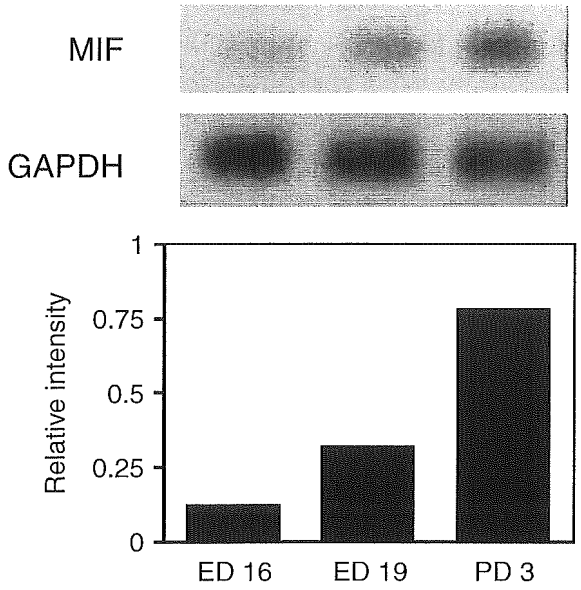

Figure 3. Northern blot analysis of macrophage migration inhibitory factor (MIF) mRNA in embryonic day (ED) 16, 19, and postnatal day (PD) 3 skin. Whole skin (epidermis plus dermis) was subjected to Northern blot analysis as described in the *Materials and methods* section. The densities of MIF bands were normalized to the glyceraldehyde-3-phosphate dehydrogenase (GAPDH) signals. MIF mRNA was first detected on ED 16 skin. MIF mRNA was markedly up-regulated on PD 3 skin.

mesenchymal cells (19). These observations are consistent with the timing of MIF mRNA expression and support the idea that MIF is also involved in the generation of dermal cells such as dermal papilla cells which are able to induce hair follicle progression and development (20). In the present study, MIF mRNA expression levels were detected in the hair germ at ED 16 at the start of hair bud formation.

MIF is expressed in highly proliferative tissues such as the corneal epithelium (21), osteoblasts (22), leukemia cells (23), and the early embryonic chicken lens (24). Expression of MIF in rat brain during fetal development was examined using *in situ* hybridization (7). It is hypothesized that MIF expression may be involved in the generation of both neurons and glial cells (7). Besides the central nervous system, MIF may play an important role in the development of the chicken lens in the eye, where MIF mRNA expression correlates with differentiation of lens cells (24). Moreover, MIF mRNA was also expressed in ovulated ooctyes, zygotes, the two-cell embryo, eight-cell embryo stages, and blastocysts (25). Conversely, targeted disruption of the MIF gene in mice causes no detectable developmental abnormalities (26,27). However, morpholino oligomer-mediated knockdown of MIF caused a severely altered phenotype, which demonstrated that MIF is an essential factor in Xenopus embryogenesis, and suggested the importance of mammalian MIF in the development of mammals (28). A detailed MIF expression pattern during mouse embryogenesis was also reported (29). The report suggests the involvement of MIF in the development of various tissues, although skin development was not proposed (29). Although the precise molecular function of MIF in skin development remains to be elucidated, these findings support the general idea that significant MIF expression may be directly or indirectly associated with the development of epidermis and hair follicles.

Table 1. Summary of macrophage migration inhibitory factor mRNA expression in developing rat skin

Stage	Epidermis	Hair follicle
ED 13	–	–
ED 16	+	–
ED 19	+	+
PD 3	++	++

–, negative; +, positive; ++, strongly positive; ED, embryonic day; PD, postnatal day.

Acknowledgements

This research was supported by a Grant-in-Aid for research (No. 11670813 and 13357008) from the Ministry of Education, Science, and Culture of Japan. We thank Dr James R. McMillan for proofreading this manuscript.

References

1. Calandra T, Bernhagen J, Mitchell R A, Bucala R. The macrophage is an important and previously unrecognized source of macrophage migration inhibitory factor. J Exp Med 1994: 179: 1895–1902.
2. Lanahan A, Williams J B, Sanders L K, Nathans D. Growth factor-induced delayed early response genes. Mol Cell Biol 1992: 12: 3919–3929.
3. Imamura K, Nishihira J, Suzuki M et al. Identification and immunohistochemical localization of macrophage migration inhibitory factor in human kidney. Biochem Mol Biol Int 1996: 40: 1233–1242.
4. Bernhagen J, Calandra T, Mitchell R A et al. MIF is a pituitary-derived cytokine that potentiates lethal endotoxaemia. Nature 1993: 365: 756–759.
5. Shimizu T, Ohkawara A, Nishihira J, Sakamoto W. Identification of macrophage migration inhibitory factor (MIF) in human skin and its immunohistochemical localization. FEBS Lett 1996: 381: 188–202.
6. Suzuki T, Ogata A, Tashiro K et al. A method for detection of a cytokine and its mRNA in the central nervous system of the developing rat. Brain Res Brain Res Protoc 1999: 4: 271–279.
7. Suzuki T, Ogata A, Tashiro K, Nagashima K, Tamura M, Nishihira J. Augmented expression of macrophage migration inhibitory factor (MIF) in the telencephalon of the developing rat brain. Brain Res 1999: 16: 457–462.

8. Hirota S, Ito A, Morii E et al. Localization of mRNA for c-kit receptor and its ligand in the brain of adult rats: an analysis using in site hybridization histochemistry. Brain Res Mol Brain Res 1992: 15: 47–54.
9. Bloom B R, Bennett B. Mechanism of a reaction in vitro associated with delayed-type hypersensitivity. Science 1966: 153: 80–82.
10. Shimizu T. Role of macrophage migration inhibitory factor (MIF) in the skin. J Dermatol Sci 2005: 37: 65–73.
11. Bernhagen J, Bacher M, Calandra T et al. An essential role for macrophage migration inhibitory factor in the tuberculin delayed-type hypersensitivity reaction. J Exp Med 1996: 183: 277–282.
12. Calandra T, Bernhagen J, Metz C N et al. MIF as a glucocorticoid-induced modulator of cytokine production. Nature 1995: 377: 68–71.
13. Bacher M, Metz C N, Calandra T et al. An essential regulatory role for macrophage migration inhibitory factor in T-cell activation. Proc Natl Acad Sci USA 1996: 93: 7849–7854.
14. Abe R, Shimizu T, Ohkawara A, Nishihira J. Enhancement of macrophage migration inhibitory factor (MIF) expression in injured epidermis and cultured fibroblasts. Biochim Biophys Acta 2000: 1500: 1–9.
15. Shimizu T, Nishihira J, Watanabe H et al. Macrophage migration inhibitory factor (MIF) is induced by thrombin and factor Xa in endothelial cells. J Biol Chem 2004: 279: 13729–13737.
16. Shimizu T, Abe R, Ohkawara A, Nishihira J. Ultraviolet B radiation up-regulates the production of macrophage migration inhibitory factor (MIF) in human epidermal keratinocytes. J Invest Dermatol 1999: 112: 210–215.
17. Leukert N, Sorg C, Roth J. Molecular basis of the complex formation between the two calcium-binding proteins S100A8 (MRP8) and S100A9 (MRP14). Biol Chem 2005: 386: 429–434.
18. Oomizu S, Sahuc F, Asahina K et al. Kdap, a novel gene associated with the stratification of the epithelium. Gene 2000: 256: 19–27.
19. Osada A, Kobayashi K. Appearance of hair follicle-inducible mesenchymal cells in the rat embryo. Dev Growth Differ 2000: 42: 19–27.
20. O'Shaughnessy R F, Christiano A M, Jahoda C A. The role of BMP signalling in the control of ID3 expression in the hair follicle. Exp Dermatol 2004: 13: 621–629.
21. Matsuda A, Tagawa Y, Matsuda H, Nishihira J. Expression of macrophage migration inhibitory factor in corneal wound healing in rats. Invest Ophthalmol Vis Sci 1997: 38: 1555–1562.
22. Onodera S, Suzuki K, Matsuno T, Kaneda K, Kuriyama T, Nishihira J. Identification of macrophage migration inhibitory factor in murine neonatal calvariae and osteoblasts. Immunology 1996: 89: 430–435.
23. Nishihira J, Koyama Y, Mizue Y. Identification of macrophage migration inhibitory factor in human leukemia HL-60 cells and its induction by lipopolysaccharide. Biochem Mol Biol Int 1996: 40: 861–869.
24. Wistow G J, Shaughnessy M P, Lee D C, Hodin J, Zelenka P S. A macrophage migration inhibitory factor is expressed in the differentiating cells of the eye lens. Proc Natl Acad Sci USA 1993: 90: 1272–1275.
25. Suzuki H, Kanagawa H, Nishihira J. Evidence for the presence of macrophage migration inhibitory factor in murine reproductive organs and early embryos. Immunol Lett 1996: 51: 141–147.
26. Bozza M, Satoskar A R, Lin G et al. Targeted disruption of migration inhibitory factor gene reveals its critical role in sepsis. J Exp Med 1999: 189: 341–346.
27. Honma N, Koseki H, Akasaka T et al. Deficiency of the macrophage migration inhibitory factor gene has no significant effect on endotoxaemia. Immunology 2000: 100: 84–90.
28. Suzuki M, Takamura Y, Maeno M et al. Xenopus laevis macrophage migration inhibitory factor is essential for axis formation and neural development. J Biol Chem 2004: 279: 21406–21414.
29. Kobayashi S, Satomura K, Levsky J M et al. Expression pattern of macrophage migration inhibitory factor during embryogenesis. Mech Dev 1999: 84: 153–156.

+Model

Available online at www.sciencedirect.com
SCIENCE DIRECT®

ELSEVIER

Colloids and Surfaces A: Physicochem. Eng. Aspects xxx (2005) xxx–xxx

COLLOIDS AND SURFACES A

www.elsevier.com/locate/colsurfa

Effect of honeycomb film on protein adsorption, cell adhesion and proliferation

Hiroshi Sunami[a,*], Emiko Ito[b], Masaru Tanaka[a,b], Sadaaki Yamamoto[a,b], Masatsugu Shimomura[b,c]

[a] *Creative Research Initiative "Sousei" (CRIS), Hokkaido University, Hokkaido, Japan*
[b] *CREST, Japan Science and technology Corporation (JST), Japan*
[c] *Nanotechnology Research Center, Research Institute for Electronic Science, Hokkaido University, Hokkaido, Japan*

Received 1 November 2005; received in revised form 8 November 2005; accepted 10 November 2005

Abstract

This article describes novel methods for controlling of cell adhesion by using micro porous polymer films. Recently we found the highly ordered micro porous films were formed when poly(ε-caprolactone) (PCL) solution was cast on substrates at high atmospheric humidity. The micro porous film has regular honeycomb morphology with a size of 5 μm per cell (honeycomb film). Endothelial cells grew rapidly on the honeycomb film. After 24 h cell culture, the cell number on honeycomb films was lager than that on PCL flat films. In order to elucidate the effect of honeycomb films as a scaffold for cell culture, the adsorbed proteins on honeycomb films under cell culture condition were observed. After conditioning of the honeycomb film and the flat film in DMEM containing 10% foetal bovine serum (FBS) for 72 h at 37 °C in 5% CO_2 atmosphere, the adsorbed fibronectin-FITC and albumin-Texasred on the honeycomb films was observed by using confocal laser scanning microscope (CLSM). The observation revealed that fibronectin showed site-selective adsorption behavior on the honeycomb film. Albumin adsorbed on the honeycomb film non site-selectively, while fibronectin mainly adsorbed on inside of honeycomb pores. On the flat film, fibronectin was hardly observed. Since the honeycomb film accelerate the adsorption of fibronectin which is a typical protein as a cell adhesion molecule, the film could be a scaffold with excellent cell adhesion properties.

Keywords: Honeycomb film; Cell adhesion; Cell proliferation; Fibronectin; Tissue engineering; Self-organization

1. Introduction

Cell behaviors such as growth, apoptosis and differentiation are controlled by micro-patterned cell adhesive surface [1–3]. Therefore, micro-patterning of cell adhesive regions attracts much attention. A large number of methods for preparing micro-patterned cell adhesive surface have been developed by photolithography and related techniques [1–18].

We have reported that micrometer size patterned polymer film (honeycomb film) can be prepared by self-organization [19]. The honeycomb film possessing a hexagonal array of micropores could be obtained by solution casting of various types of polymers on a solid substrate in a humid atmosphere. This method is simple and does not require special instrumentation in comparison with the photolithography method. Recently, we reported that honeycomb film could be utilized for the micropatterned cell culture substrate [20–22]. The honeycomb film can modulate cell adhesion and concomitant behavior such as morphological change and expression of cell function [23–26]. In order to elucidate the effect of honeycomb films as a scaffold for cell culture, the adsorbed proteins on honeycomb films under cell culture condition were observed. Since adsorption of proteins on substrates is thought to be an initial process for cell adhesion and growth, it is important to reveal the protein adsorption on honeycomb film. In this research, adsorbed proteins on honeycomb films were determined by immunostaining, and their topological structure were observed by confocal laser scanning microscopy.

2. Experiment

The honeycomb film was fabricated by applying a moist air to a spread polymer solution containing biodegradable

* Corresponding author. Tel.: +81 11 706 9255
E-mail address: sunami@poly.es.hokudai.ac.jp (H. Sunami).

0927-7757/$ – see front matter © 2005 Elsevier B.V. All rights reserved.
doi:10.1016/j.colsurfa.2005.11.041

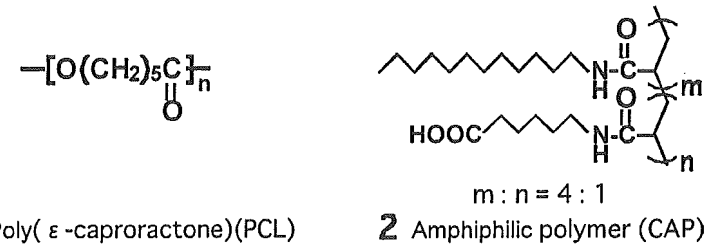

1 Poly(ε -caproractone)(PCL) 2 Amphiphilic polymer (CAP)

Scheme 1.

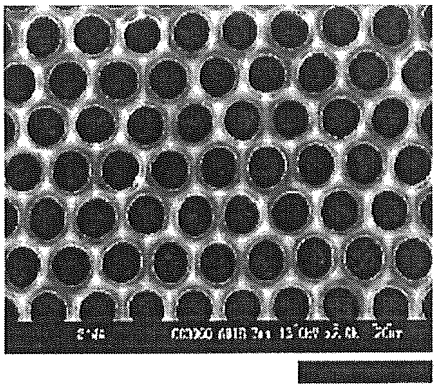

Fig. 1. SEM image of honeycomb film (PCL, pore size 5 μm).

polymers (poly(ε-caprolactone) (PCL)) 1 and an amphiphilic polymer (co-carboxyhexyl acrylamide (CAP)) 2 (10:1 wt.%) (Scheme 1). A chloroform solution (5 mg/ml) containing PCL (MW = 70,000–100,000) and CAP (MW = 20,000) were used. Evaporative cooling lead to the formation of hexagonally-packed water droplets on the polymer solution. The honeycomb structure with pore diameter of 5 μm and a wall thickness of 8 μm was prepared on disk-type cover grass (Ø 15 mm) (Fig. 1). Flat films made from the same materials, were prepared as a reference. These honeycomb films and flat films were immersed in 1-propanol for 12 min to remove the CAP.

After conditioning (pre-incubation) of the honeycomb films and the flat films in Dulbecco's modified Eagle's minimal essential medium (DMEM; SIGMA Co. Ltd, St. Louis, MO, USA) supplemented with 10% heat-inactivated fetal bovine serum (FBS; Thermo Trace Ltd., Melbourne, Australia) and 1% Penicillin–Streptomycin (Gibco, Grand Island, NY, USA) for 72 h at 37 °C in 5% CO_2 atmosphere, adsorbed fibronectin-FITC and albumin-Texas red on the honeycomb films was observed in PBS by using confocal laser scanning microscope (FV-300, Olympus. Co., Tokyo, Japan). Fibronectin and albumin in the FBS previously were immunostained by anti-fibronectin FITC conjugate (Biogenesis Ltd., UK) and anti-albumin Texas red conjugate (Rockland immunochemicals, Inc., USA).

Porcine aortic endothelial cells (ECs, passage 2) were purchased from DAINIPPON PHARMACEUTICAL Co., Ltd. The honeycomb films and the flat films were insert to 24-well plates (IWAKI Microplate; IWAKI Glass Co., Funahashi, Japan). The ECs were used at passage 6 to seed the 24-well plate at a concentration of 1.5×10^4 cells/cm^2 (cells/ml) in 1 ml DMEM supplemented with 10% FBS and 1% Penicilli–Streptomycin.

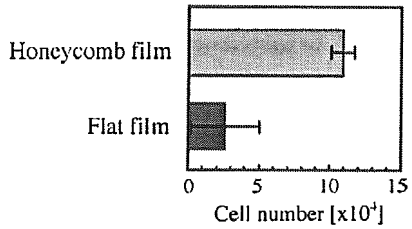

Fig. 3. Number of ECs on honeycomb film and on flat film after 24 h incubation.

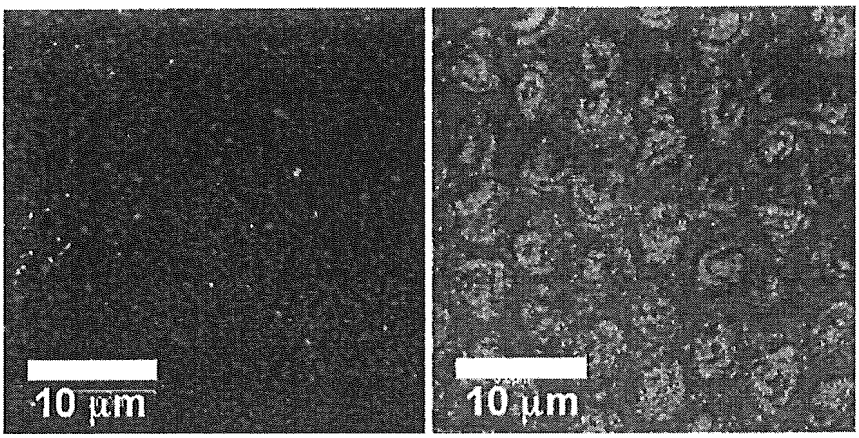

Fig. 2. Fluorescence images of adsorbed protein after 72 h conditioning on flat film and on honeycomb film. Green points are adsorbed fibronectin. Red points are adsorbed albumin.

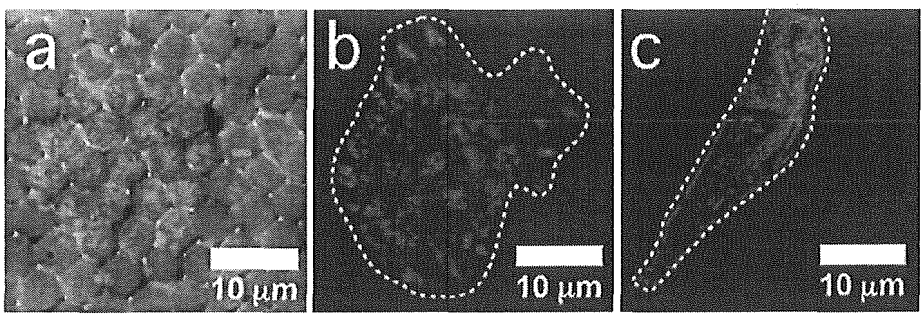

Fig. 4. (a) Superposition image between differential interference image of honeycomb film and immnostained vinculin of EC on the honeycomb film. Comparison of focal adhesion points of EC between on (b) honeycomb film and (c) flat film. White dots are outline of an EC. Red points are immnostained vinculin cluster (Alexa Fluor 546).

After 24 h the ECs culture, the number on the each substrate was evaluated with the Cell Proliferation Reagent WST-1 (F. Hoffmann-La Roche Ltd., Basel, Switzerland). All cell cultures were maintained in a humidified incubator at 37 °C in 5% CO_2/95% air.

After 24 h on the substrates, cells were washed with PBS and fixed with 10% formalin in PBS for 10 min. The cells were made permeable with 1% Triton-X for 30 min, washed with 0.05% T-PBS for 5 min, and incubated with a 1:100 dilution of mouse anti-vinculin monoclonal antibody (CHEMICON international, Inc., Temecula, CA, USA), respectively, for 90 min at 37 °C. After washed with 0.05% T-PBS for 5 min, the cells were labeled with a 1:1000 dilutions of Alexa Fluor 546 rabbit anti-goat IgG (Molecular Probes, Inc., Eugene, OR, USA) in PBS for 60 min at 37 °C. The cells were visualized with the confocal laser scanning microscope (FV-300, Olympus. Co., Tokyo, Japan).

3. Results and discussion

After 72 h conditioning, the fluorescence images of the adsorbed fibronectin-FITC and the albumin-Texas red on the honeycomb films and the flat films are shown in Fig. 2. The observation revealed that the fibronectins show characteristic adsorption behavior on the honeycomb film. However, the fibronectins (green points) hardly adsorbed on the flat films, the large amount of fibronectin adsorbed on the honeycomb film. Albumin (red points) adsorbed on the honeycomb film non site-selectively, while fibronectin mainly adsorbed on inside of honeycomb pores. It should be noted that clearly difference was observed for the adsorbed fibronectin structure between the honeycomb films and the flat films, although the surface chemical compositions are the same.

After 24 h incubation, the number of ECs on the honeycomb film was compared with that of ECs on the flat film (Fig. 3). The cell number on the honeycomb films was nearly four times lager than that on the flat films. The honeycomb film is expected to be a good scaffold for an EC culture system, because the honeycomb film could accelerate the EC proliferation.

The cell proliferation is highly regulated by cell-adhesion behavior onto biomaterials. Focal adhesion, which plays a crucial role in cell-adhesion behavior, is major cellular sites responsible for cell–protein attachment. The focal adhesion points (vinculin cluster) are mainly observed in inside of honeycomb pores (Fig. 4a). The site-selective distribution of focal adhesion points indicates that ECs adhere to adsorbed fibronectin molecules in the honeycomb pores. The morphology of focal adhesion points was clearly different between the honeycomb film (Fig. 4b) and the flat film (Fig. 4c), it was suggested that the difference of cell proliferation properties between these films is caused by the difference of focal adhesion points. The honeycomb film can control cell adhesion and proliferation by regulating the protein adsorption. This makes honeycomb film effective cell culture scaffold with high adhesion properties.

4. Conclusion

We reported that the site-selectively fibronectin adsorbed honeycomb film plays vital roles in cell adhesion and proliferation. The honeycomb film was demonstrated influencing cellular attachment and growth via the site-selective adsorption structure of fibronectin molecules. Hence, the honeycomb film could be an excellent scaffold with accelerating properties of cell adhesion and proliferation. These results indicate that a new method of controlling the protein adsorption, and, ultimately mediating cell adhesion and cell proliferation by using honeycomb film.

Acknowledgements

We are grateful for the funding for this work provided by "Special Coordination Funds for Promoting Science and Technology" of Ministry of Education, Culture, Sports, Science and Technology, and CREST, Japan Science and technology Corporation (JST).

References

[1] R. Singhvi, A. Kumar, G.P. Lopez, G.N. Stephanopoulos, D.I.C. Wang, G.M. Whitesides, D.E. Ingber, Science 264 (1994) 696.
[2] C.S. Chen, M. Mrksich, S. Huang, G.M. Whitesides, D.E. Ingber, Science 276 (1997) 1425.
[3] S.N. Bhatia, M.L. Yarmush, M. Toner, J. Biomed. Mater. Res. 34 (1997) 189.
[4] B. Lom, K.E. Healy, P.E. Hochberger, J. Neurosci. Methods 50 (1993) 385.

[5] D.V. Nicolau, T. Taguchi, H. Taniguchi, S. Yoshikawa, Langmuir 15 (1999) 3845.
[6] S.P.A. Fodor, J.L. Read, M.C. Pirrung, L. Stryer, A.T. Lu, D. Solas, Science 251 (1991) 767.
[7] D.J. Pritchard, H. Morgan, J.M. Cooper, Angew. Chem. Soc. 114 (1999) 4432.
[8] T. Matsuda, T. Sugawara, Langmuir 11 (1995) 2272.
[9] S.K. Bhatia, J.J. Hickman, F.S. Ligler, J. Am. Chem. Soc. 114 (1992) 4432.
[10] D.A. Stenger, J.H. Georger, C.S. Dulcey, J.J. Hickman, A.S. Rudolph, T.B. Nielsen, S.M. McCort, H.M. Calvert, J. Am. Chem. Soc. 114 (1992) 8435.
[11] C.S. Dulcey, J.H.J. Georger, V. Krauthamer, D.A. Stenger, T.L. Fare, J.M. Calvert, Science 252 (1991) 551.
[12] M. Matsuzawa, K. Umemura, D. Beyer, K. Sugioka, W. Knoll, Thin Solid Films 305 (1997) 74.
[13] J. Lahiri, E. Ostuni, G.M. Whitesides, Langmuir 15 (1999) 2055.
[14] L.A. Kung, L. Kam, J.S. Hovis, S.G. Boxer, Langmuir 16 (2000) 6773.
[15] A. Barnard, J.P. Penault, B. Michel, H.R. Bosshard, E. Delamarche, Adv. Mater. 12 (2000) 1067.
[16] M. Mrksich, G.M. Whitesides, Annu. Rev. Biophys. Biomol. Struct. 25 (1996) 55.
[17] S. Takayama, J.C. McDonald, E. Ostuni, M.N. Liang, P.J.A. Kents, R.F. Ismaginov, G.M. Whitesides, Proc. Natl. Acad. Sci. U.S.A. 96 (1999) 5545.
[18] E. Delamarche, A. Bernard, H. Schmid, B. Michel, H. Biebuyck, Science 276 (1997) 779.
[19] N. Maruyama, T. Koito, J. Nishida, T. Sawadaishi, X. Cieren, K. Ijiro, O. Karthaus, M. Shimomura, Thin Solid Films 327–329 (1998) 854.
[20] T. Nishikawa, J. Nishida, R. Ookura, S. Nishimura, S. Wada, T. Karino, M. Shimomura, Mater. Sci. Eng. C 8–9 (1999) 495.
[21] T. Nishikawa, J. Nishida, R. Ookura, S. Nishimura, S. Wada, T. Karino, M. Shimomura, Mater. Sci. Eng. C 10 (1999) 141–146.
[22] J. Nishida, K. Nishikawa, S.-I. Nishimura, S. Wada, T. Karino, T. Nishikawa, K. Ijiro, M. Shimomura, Polym. J. 34 (3) (2002) 166–174.
[23] K. Sato, M. Tanaka, M. Takebayashi, K. Nishikawa, M. Shimomura, Int. J. Nanosci. 1 (5&6) (2002) 689–693.
[24] M. Tanaka, M. Takebayashi, M. Miyama, J. Nishida, M. Shimomura, Bio-Med. Mater. Eng. 14 (2004) 439–446.
[25] A. Tsuruma, M. Tanaka, N. Fukushima, M. Shimomura, e-J. Surf. Sci. Nanotechnol. 3 (2005) 159–164.
[26] T. Nishikawa, J. Nishida, K. Nishikawa, R. Ookura, H. Ookubo, H. Kamachi, M. Matsushita, S. Todo, M. Shimomura, Stud. Surf. Sci. Catal. 132 (2001) 509–512.